

Article

Synthesis, Structure, and Catalytic Reactivity of Pd(II) Complexes of Proline and Proline Homologs

David B. Hobart Jr. , Joseph S. Merola * , Hannah M. Rogers, Sonia Sahgal, James Mitchell, Jacqueline Florio and Jeffrey W. Merola

Department of Chemistry, Virginia Tech, Blacksburg, VA 24061, USA; dhobart@vt.edu (D.B.H.J.); hannahm@vt.edu (H.M.R.); sonia.sahgal5@gmail.com (S.S.); jhmvmt@gmail.com (J.M.); jflo5392@vt.edu (J.F.); senrath@gmail.com (J.W.M.)

* Correspondence: jmerola@vt.edu

Received: 7 May 2019; Accepted: 6 June 2019; Published: 10 June 2019



Abstract: Palladium(II) acetate reacts with proline and proline homologs in acetone/water to yield square planar bis-chelated palladium amino acid complexes. These compounds are all catalytically active with respect to oxidative coupling of olefins and phenylboronic acids. Some enantioselectivity is observed and formation of products not reported in other Pd(II) oxidative couplings is seen. The crystal structures of nine catalyst complexes were obtained. Extended lattice structures arise from N-H•••O or O••(HOH)•••O hydrogen bonding. NMR, HRMS, and single-crystal XRD data obtained on all are evaluated.

Keywords: palladium; chelate; amino acid; proline; N-methylproline; azetidine; pipercolinic acid; 4-fluoroproline; 4-hydroxyproline; 2- α -benzylproline; hydrogen bonding; oxidative coupling; X-ray crystallography

1. Introduction

Oxidative coupling reactions are some of the most utilized reactions in modern synthetic chemistry, and transition metal catalyzed oxidations are well known [1]. Palladium(II) oxidative coupling catalysis is a huge field [1–6], and this introduction cannot give even a cursory overview of it [7–13]. Some recent reviews may be the best way of relaying important background information. Focusing on the general, reactions such as the Heck, Suzuki, and Sonogashira couplings are known to proceed via a Pd⁰ species, with oxidative addition/reductive elimination yielding the desired products. Oxidative palladium(II) catalysis differs from these in that it utilizes molecular oxygen to regenerate the active catalyst in palladium(II) catalyzed coupling reactions. There are two proposed mechanisms for the catalytic cycle [14–20].

There are many different types of coupling reactions noted to proceed via palladium(II) oxidative catalysis. There are hundreds of examples in the current literature of carbon-carbon [2,5,21–39], carbon-oxygen [40–47], carbon-nitrogen [47–55], carbon-sulfur [42,56,57], and carbon-phosphorous [58] couplings that are catalyzed by palladium(II) oxidative catalysis. These coupling reactions are used in the manufacture of many pharmaceuticals, natural products, fine chemicals, and polymers. In addition, palladium catalysts are known for their functional group tolerance, mild reaction conditions, and low sensitivity to air and water. Pairing these advantages with an abundant and easily accessible oxidant source shows the great utility and economic benefit that these systems can provide.

Also important for this discussion is a significant history of using amino acids as chelating ligands, especially for Pd(II) and Pt(II). Wolfgang Beck has had a five-decade career publishing the series “Metal Complexes of Biologically Important Ligands,” consisting of over 175 articles [59]. Many of those papers deal with amino acid complexes of metals including palladium. Recently, proline has

come to the fore as a “co-catalyst” used along with palladium in a number of organic reactions [60]. More specifically related to this paper are recent publications that describe a bis-proline complex of palladium as catalyst for various organic transformations. Blum et al. [61] show that proline complexes of Pd(II) catalyze various coupling reactions, while Chatterjee et al. [62] showed that bis-proline Pd(II) complexes were useful in the Suzuki-Miyaura cross-coupling reaction in water. The formation of biaryl products from palladium-catalyzed cross-couplings is well known, and there are examples from the literature [21,50,63–67] that demonstrate that these biaryls can be formed as desired reaction products or as undesired side products. For reactions where the cross-coupled product is desired, the formation of biaryls is an unwanted side reaction and catalyst systems of this type where the biaryl formation is minimized or eliminated are preferred.

This paper describes the synthesis and catalytic activity of palladium(II)-amino acid chelates where proline, N-methylproline, 4-fluoroproline, 4-hydroxyproline, 2-benzylproline, azetidine-2-carboxylic acid, and pipercolinic acid were used as the chelating ligands. In earlier work, we showed that the amino acid complexes of rhodium and iridium piano stools were useful for asymmetric hydrogenation [68]. We have previously reported on the simpler glycine complexes [69], and these proline and proline homologs represent another unique subset of amino acid ligands where the R-group of the amino acid is a cyclic ring moiety. Subsequent papers will discuss our work with beta-amino acid complexes and amino acids where the R-group is a linear substituent.

2. Results and Discussion

2.1. Characterization and Hydrogen Bonding Interactions

In the following discussions, compounds **1–9** (Figure 1, above) were synthesized as shown in the reaction scheme in Figure 2:

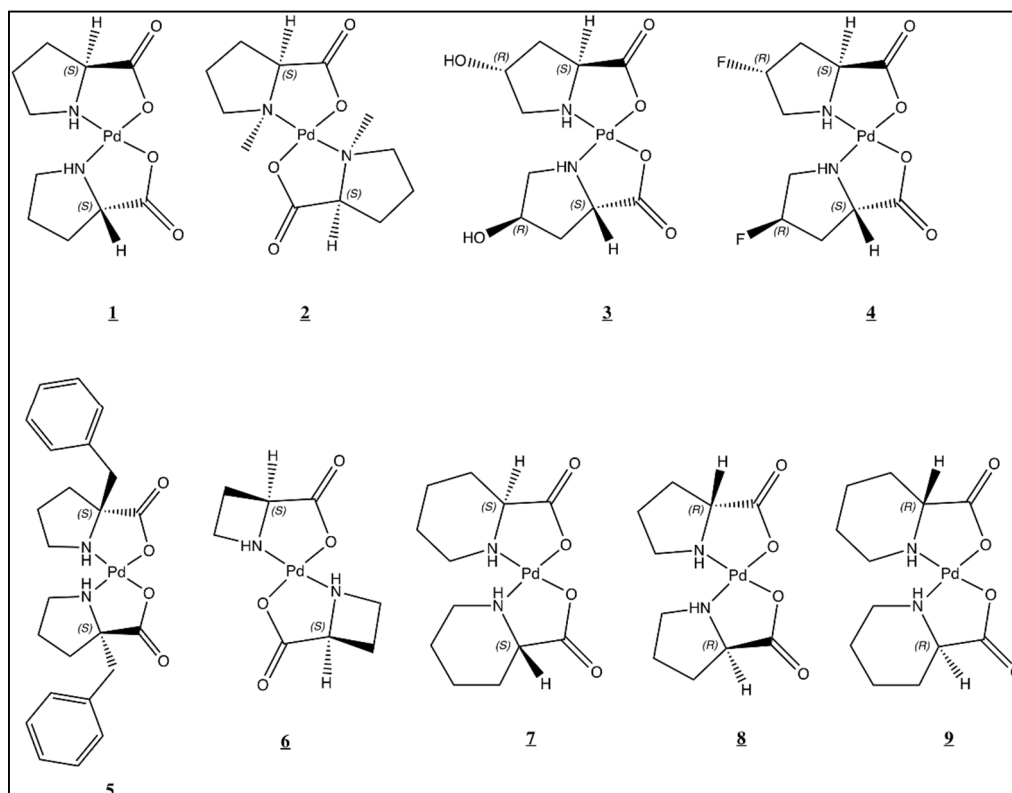


Figure 1. Compound structures and numbering scheme for proline and proline homolog complexes. Stereochemistry is shown at all chiral centers.

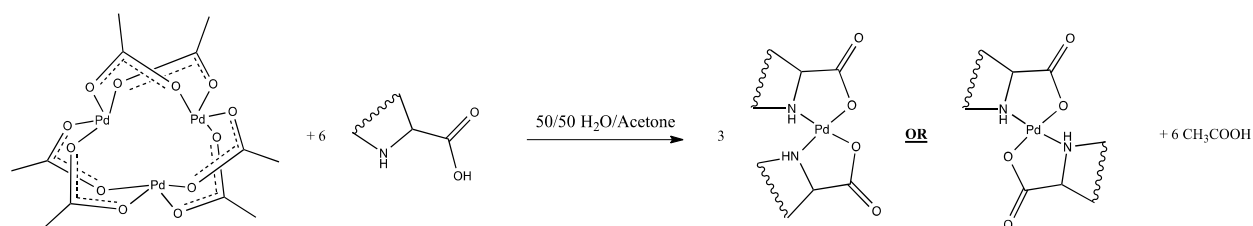


Figure 2. General reaction scheme for the synthesis of *cis* and *trans* palladium(II) proline/cyclic complexes.

The most common of the cyclic amino acids is L-proline, one of 20 naturally occurring α -amino acids. Compound **1** was prepared as the *cis* isomer and confirmed by X-ray crystal structure analysis (Figure 3).

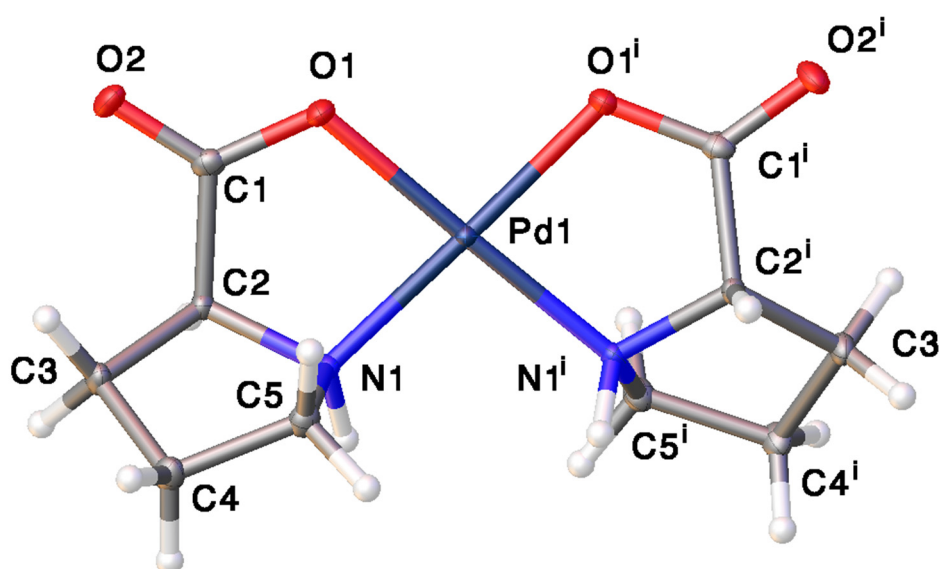


Figure 3. Thermal ellipsoid plot of the molecular structure of crystalline *cis*-bis(L-prolinato)palladium(II), **1**. Atoms labelled “i” are generated by a C_2 rotation. Thermal ellipsoids are shown at the 50% probability level. CCDC:1913626.

The complex crystallizes in the $C222_1$ space group. Pd-N and Pd-O bond lengths are 2.0105 Å and 2.0193 Å, respectively. N-Pd-O bond angles are 82.65° for each chelate ring and 96.27° between the chelate rings (O-Pd-O). There were no unusual bond lengths and angles in complex **1** (see the Supplementary Materials for the full listing). Intermolecular hydrogen bonding is common for palladium amino acid complexes; the exact nature is dependent on the amino acid and any substitution on the amino acid backbone. For complex **1**, intermolecular hydrogen bonding is observed in the crystal lattice between the amine protons and the non-coordinated carboxyl oxygen atoms (Figure 4). In this case, the palladium complex molecules arrange themselves and can approach closely enough for this purely complex to complex H-bonding. This compound was reported previously by Ito et al., but at room temperature in a non-standard space group [70]. The bond lengths and angles of the compounds reported here may be compared with those reported previously in the literature [71–74].

The ^1H NMR spectrum in D_2O shows three multiplets at δ 4.08–3.63, 3.37–2.73, and 2.28–1.52, with integrated ratios of 1:2:4, respectively. Palladium’s isotope distribution pattern was observed in the HRMS spectrum (see Supplementary Materials).

D-proline was used to prepare *cis*-bis(D-prolinato)palladium(II), compound **8**. Characterization data for **8** was the same as that seen for **1**, with the stereochemistry of the chiral carbon reversed (see Supplementary Materials), as is expected for enantiomeric species.

In *N*-methylproline the amine proton in proline is replaced with a methyl group. The resultant complex formed with this ligand is *trans* bis-(*N*-methylprolinato) palladium(II) (Figure 5), confirmed by X-ray crystallographic analysis.

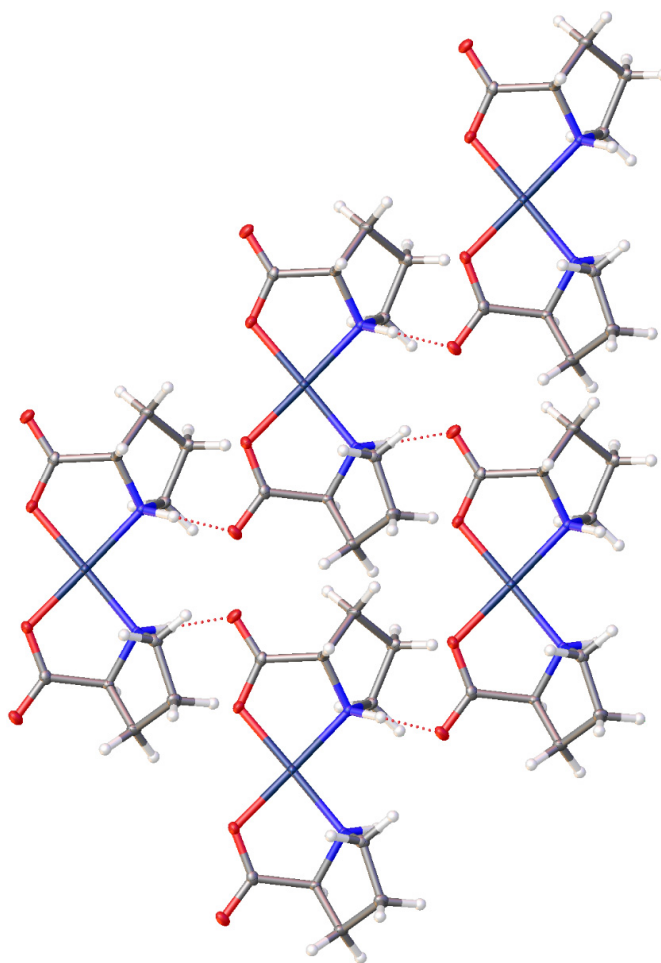


Figure 4. Crystal packing diagram for complex **1** viewed along [001] showing the intermolecular hydrogen bonding motif.

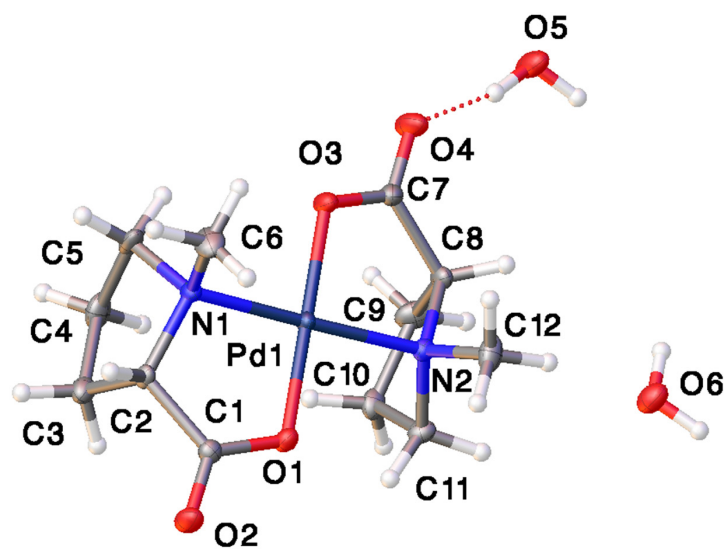


Figure 5. Thermal ellipsoid plot of the molecular structure of crystalline *trans*-bis-(*N*-methylprolinato) palladium(II) dihydrate, **2**. Thermal ellipsoids are shown at the 50% probability level. CCDC:1913622.

As with the glycine complexes, replacement of the amine hydrogen atom with a methyl group results in a degree of steric crowding that disfavors formation of the *cis* isomer [69]. All attempts to synthesize the *cis* isomer from PdCl₂ were unsuccessful. Complex **2** crystallizes in the P2₁2₁2₁ space group with Pd-N and Pd-O bond lengths of 2.051 Å and 1.9900 Å, respectively. N-Pd-O bond angles are 83.90° in the chelate ring. N-Pd-O bond angles between the chelate rings are 95.42°. There were no unusual bond lengths and angles in complex **1** (see Supplementary Materials for full listing). Because there are no H-bonding donors in the molecule due to the N-methyl substitution, there is no intermolecular hydrogen bonding between complex molecules in the lattice. However, water is now incorporated in the lattice and there is hydrogen bonding between water molecules and complex molecules (Figure 6). Intermolecular hydrogen-bonded water molecules are observed to bridge between the coordinated carboxylate oxygen atom of one complex molecule and the carbonyl oxygen of an adjacent complex molecule. It is also interesting to note that both of the pyrrolidine rings are turned down such that they are orientated towards the same face of the chelate plane.

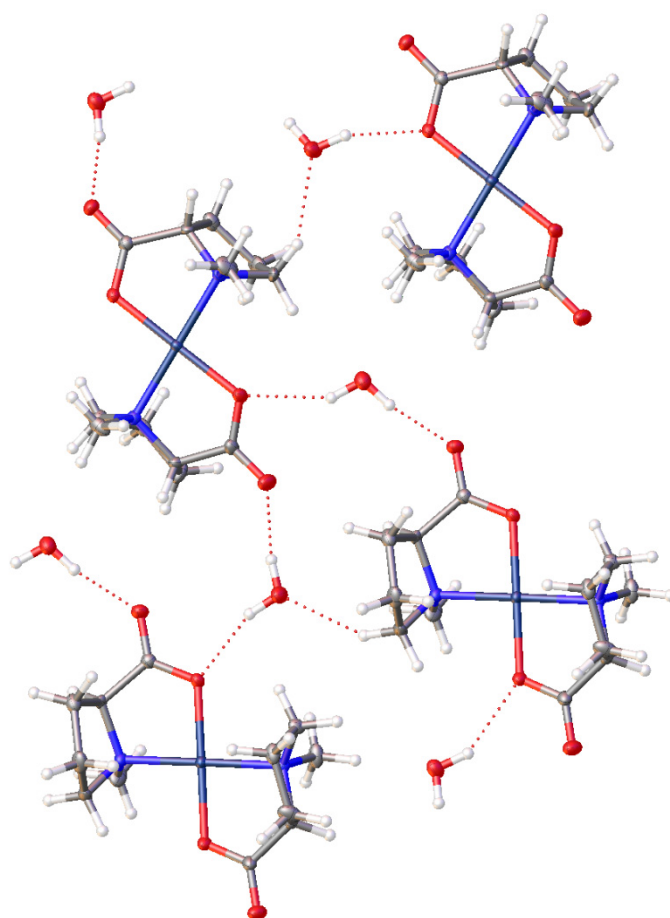


Figure 6. Crystal packing diagram of (**2**) as viewed along [010] showing the intermolecular hydrogen bonding motif.

The ¹H NMR spectrum in D₂O shows the expected singlet for the methyl protons at δ 2.71 ppm. The remaining proton resonances are present in the expected ratios; however, the splitting patterns are complex. Palladium's isotope distribution pattern is observed in the HRMS spectrum with peaks at 361.0526, 362.0542, 363.0532, 365.0531, and 367.0541 amu.

Hydroxyproline and fluoroproline have more electron-withdrawing substituents on their backbones than their strictly alkyl homologs, and this influence was probed by synthesizing their respective complexes **3** and **4**. *Cis*-bis-(*trans*-4-hydroxyprolinato)palladium(II) was synthesized (Compound **3**, Figure 7) using *trans*-4-hydroxyproline as the ligand.

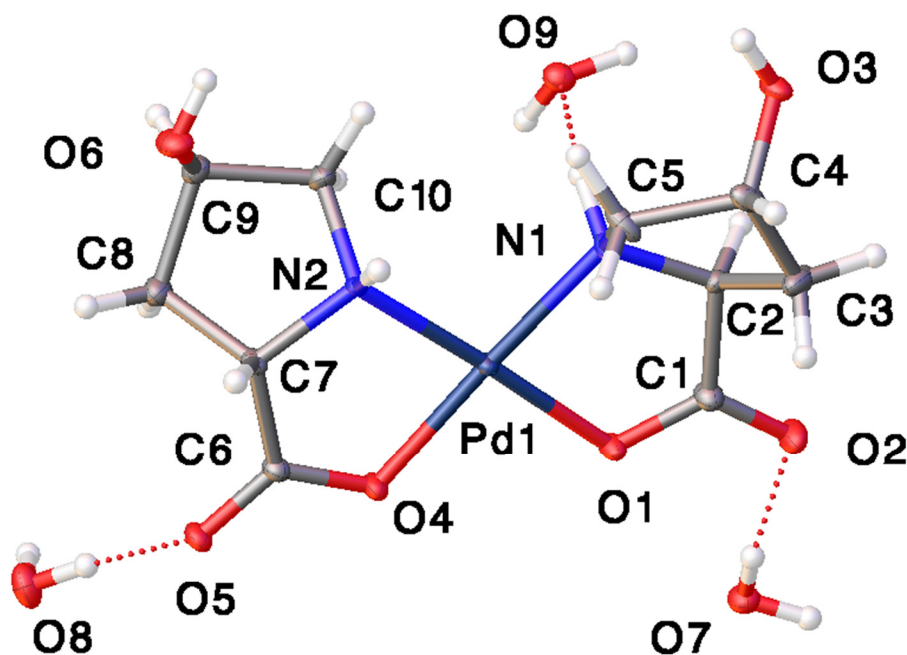


Figure 7. Thermal ellipsoid plot of the molecular structure of crystalline *cis*-bis-(*trans*-4-hydroxyprolinato)palladium(II) trihydrate, (**3**). Thermal ellipsoids are shown at the 50% probability level. CCDC:1913624.

Complex **3** crystallizes in the $P2_1$ space group with 3 hydrogen bonded water molecules per complex molecule in the lattice. The addition of another H-bond donor and acceptor complicates the H-bonding picture in the crystal lattice. There is intermolecular hydrogen bonding between one of the 4-hydroxyl group hydrogen atoms and the carbonyl oxygen of an adjacent molecule. The hydroxyl oxygen atom is hydrogen bonded to a lattice water molecule that in turn hydrogen bonds to a coordinated carboxylate oxygen of the adjacent molecule. The other 4-hydroxyl group is hydrogen bonded to two lattice water molecules that also hydrogen bond to carbonyl oxygen atoms on adjacent complex molecules in the lattice. The amine hydrogens are hydrogen bonded to lattice waters.

Pd-N and Pd-O bond lengths are 2.0153 Å and 2.0006 Å, respectively. N-Pd-O bond angles are 83.92° in the chelate ring with N-Pd-N bond angles between the chelate rings are 97.84°. All bond lengths and angles are within the ranges reported for similar d^8 metal chelates (see Supplementary Materials). The ^1H NMR spectrum in D_2O shows a singlet at 4.41 ppm, indicating that the hydroxyl proton does not exchange, or exchanges very slowly. All other resonances are as expected. Palladium's isotope distribution pattern is observed in the HRMS.

Cis-bis-(*trans*-4-fluoroprolineato)palladium(II) (Figure 8) crystallizes in the $C2$ space group. As is the case with the parent complex **1**, pure complex-to-complex H-bonding occurs and there are no water molecules in the lattice; the hydrogen bonding arrangement is quite different from that seen with the hydroxyproline complex. For the fluoroproline complex, there is hydrogen bonding from each amine hydrogen atom to a carbonyl oxygen atom on separate, adjacent complex molecules in the lattice (See Supplementary Material). The fluorine atoms do not participate in a hydrogen bonding interaction.

The Pd-N and Pd-O bond lengths in compound **4** are 2.006 Å and 2.017 Å, respectively. The N-Pd-O bond angle in the chelate ring is 82.092°, with the N-Pd-N bond angle between the chelate rings at 98.544° (see Supplementary Materials). As with the previous complexes, these values are in good agreement with other square planar palladium *N,O* chelates.

The proton NMR spectrum of complex **4** shows a complicated set of multiplets due to ^1H - ^1H and ^1H - ^{19}F coupling; however, integration does show the expected ratios of protons. The ^{13}C NMR spectrum is somewhat easier to interpret, showing the expected five carbon resonances with ^{19}F

coupling constants observed on the order of 130–170 Hz. The ^{19}F NMR shows a singlet at -179.33 ppm with ^{13}C - ^{19}F coupling of 141 Hz. HRMS shows the expected palladium isotopic pattern.

2-Benzylproline adds additional steric demands to the proline ligand. Compound **5**, *trans*-bis-(2-benzylprolinato)palladium(II) (Figure 9), was prepared using 2-benzylproline hydrochloride as the ligand.

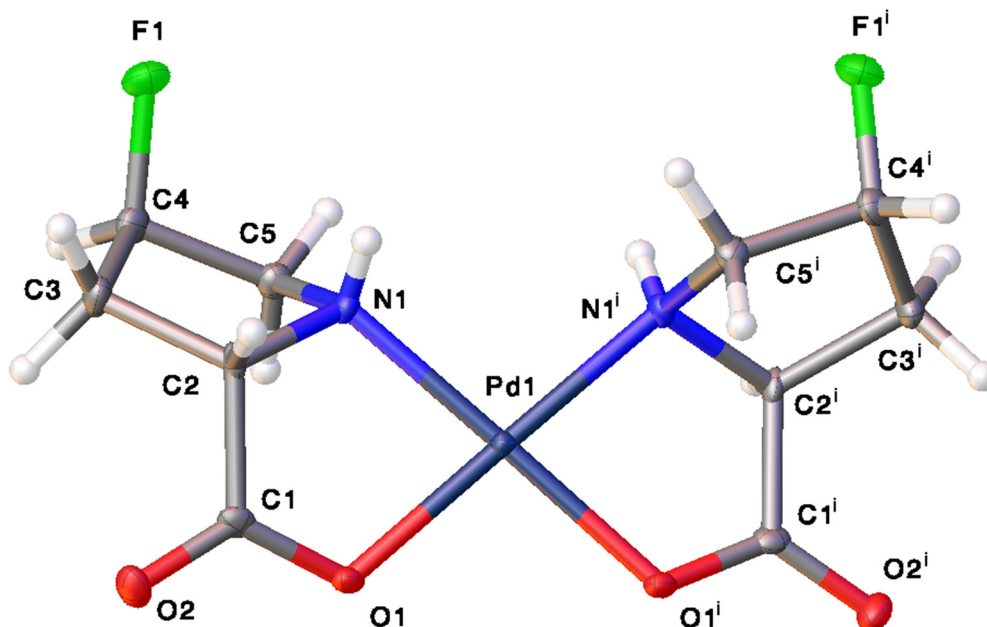


Figure 8. *Cis*-bis-(*trans*-4-fluoroprolinato)palladium(II), (**4**). Thermal ellipsoids are drawn at the 50% probability level. Atoms labeled with superscript “I” are generated by a C_2 rotation. CCDC:1913621.

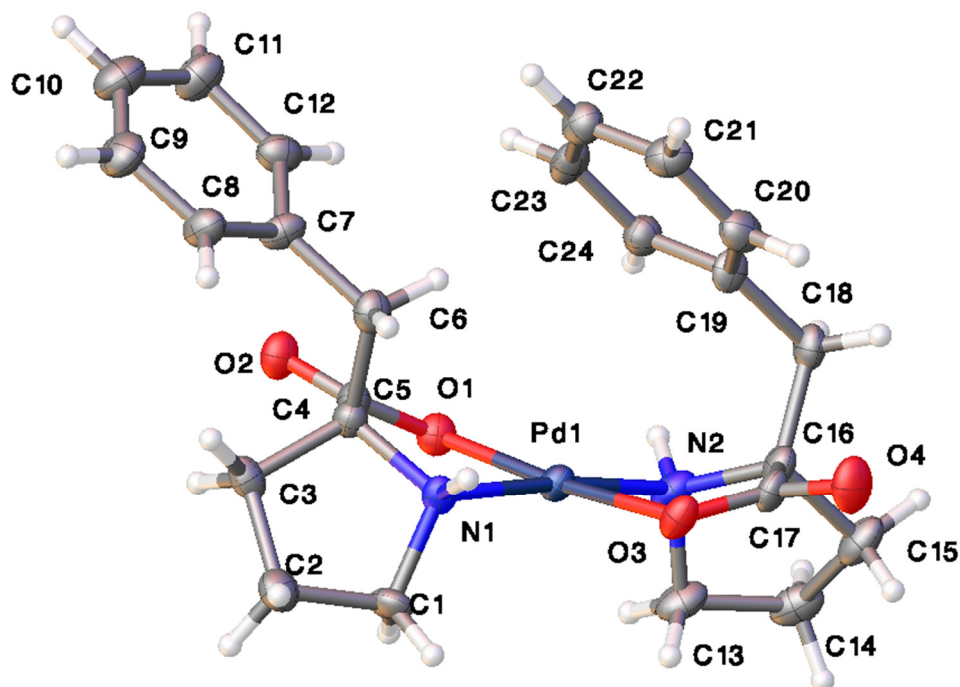


Figure 9. Thermal ellipsoid plot of the molecular structure of crystalline *trans*-bis-(2-benzylprolinato)palladium(II), **5**. Thermal ellipsoids are shown at the 50% probability level. CCDC:1913619.

Crystallizing in the $P2_12_12_1$ space group, *trans*-bis-(2-benzylprolinato)palladium(II) has Pd-N bond lengths of 2.024 Å and 2.037 Å. Pd-O bond lengths are 2.006 Å and 2.004 Å (see Supplementary Materials). The chelate rings are slightly twisted out of the square plane. The N-Pd-O angles between the chelate rings are 98.3 and 97.2°. The N-Pd-O angles in the chelate rings are 82.6°. The benzyl groups on the ligands are oriented up and away from the proline ring, with one of the benzyl groups laying over the square plane. This is the same arrangement reported by Sabat [75] for the palladium(II)-tyrosine complex; however, in the case of **5** the second benzyl group does not lie over an adjacent metal center, but rather in the lattice space between complex molecules. This arrangement does suggest that there is a π -d interaction occurring between the metal and the aromatic ring of the ligand. Two of the carbon atoms in the benzyl ring lie closer to the metal center than their calculated Van Der Waals radii. The Pd-C(19) contact distance is 3.452 Å and the Pd-C(24) contact distance is 3.472 Å. The calculated Van Der Waals radius [76] for a Pd-C bond is 3.91 Å, or approximately 0.45 Å more than what is observed in the crystal structure. This reduction in the Pd-C contact distances suggests an energetically favorable interaction between the π electron cloud of the benzyl ring and the empty d_z^2 orbital on the metal center. The other Pd-C contact distances within the benzyl ring are in the range of 4.009–4.565 Å. Hydrogen bonding occurs between the amine hydrogen atoms and the coordinated carboxylate oxygen atom of the adjacent molecule (see Supplementary Materials). There are no water molecules in the lattice, which is not surprising given the hydrophobicity of the benzyl groups.

The ^1H NMR spectrum of complex **5** is somewhat complicated. The aromatic benzyl protons show a multiplet at 7.25 ppm with the benzyl methylene protons resonating as a pair of doublets at 3.42 and 3.00 ppm. The integrated ratio of the benzyl protons is the expected 5:2. The pyrrolidine ring protons show multiplets at 3.29, 2.43, 2.02, and 1.87 ppm in a ratio of 2:1:2:1. The expected mass and isotopic splitting pattern is once again observed in the HRMS for complex **5** with the $[\text{M}+\text{H}]^+$ peak at 515.1175 amu.

The proline ring is a five-membered moiety, and both four- and six-membered ring homologs are known. The four-membered ring homolog, L-azetidine-2-carboxylic acid, was used to prepare *trans*-bis-(L-azetidine-2-carboxylato)palladium(II) (Compound **6**, Figure 10). The crystal structure of this compound shows some unique phase-change characteristics and will be the subject of a separate crystallographic paper. The ^1H NMR data show the expected ratios of integrated resonances, and the ^{13}C NMR spectrum shows possible evidence of aquo complex formation. As seen with the glycine complexes [69] discussed in a prior paper, the carbon NMR data for **6** shows two peaks for each carbon. The HRMS is as expected for a palladium complex.

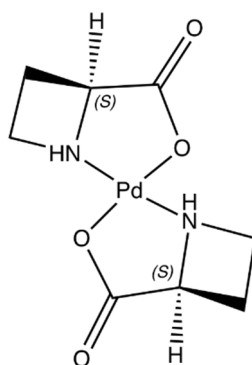


Figure 10. Molecular structure of *trans*-bis-(L-azetidine-2-carboxylato)palladium(II), (**6**).

The six-membered ring homolog, L-pipecolic acid, was used to prepare *cis*-bis-(L-pipecolinato)palladium(II) (Compound **7**, Figure 11). This complex crystallizes in the C2 space group. Pd-N and Pd-O bond lengths are approximately equivalent at 2.01–2.03 Å, comparable to the other complexes discussed within. The piperidine ring adopts the classic “chair” formation seen in cyclohexyl ring systems.

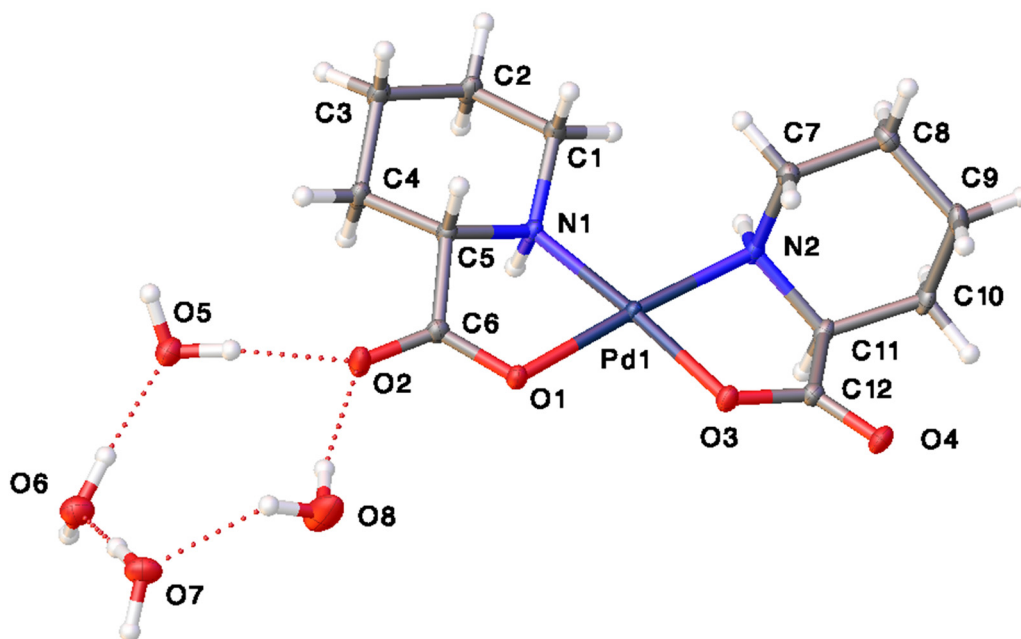


Figure 11. ORTEP plot of *cis*-bis-(L-pipecolinato)palladium(II), (**7**). Thermal ellipsoids are shown at the 50% probability level. CCDC:1913623.

There are four hydrogen bonded water molecules per complex unit in the lattice that form a pentagonal ring structure with a carbonyl oxygen of the complex. One amine hydrogen atom is hydrogen bonded to the opposite carboxyl oxygen of the adjacent molecule in the lattice. The other amine hydrogen is hydrogen bonded to one of the water molecules within the pentagonal water structure. While the specific features of these hydrogen-bonding motifs in the solid state say little about solution-state structures, they do indicate that H-bonding is most likely taking place in any solvent that contains either an H-bond donor or an H-bond acceptor or both.

D-pipecolinic acid was used to prepare *cis*-bis(D-pipecolinato)palladium(II), Compound **9**. Characterization data for **9**, as expected, is the same as that seen for **7**, but with the stereochemistry of the chiral carbon reversed (Figure 12).

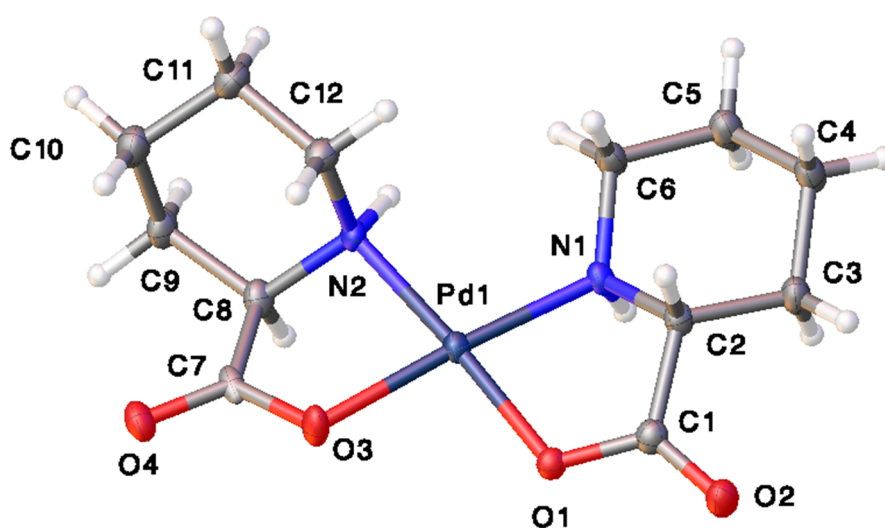


Figure 12. ORTEP plot of *cis*-bis(D-pipecolinato)palladium(II), (**9**). Lattice water molecules have been removed for clarity. Thermal ellipsoids are shown at the 50% probability level. CCDC:1913625.

2.2. Catalytic Activity

Asymmetric carbon-carbon bond formation is one of the most useful transformations in synthetic chemistry [77]. A palladium(II) catalyzed coupling reaction between phenylboronic acid and methyl tiglate was chosen as a model to evaluate the catalytic reactivity of these new palladium(II)-amino acid complexes and whether or not any asymmetric induction was possible (Figure 13).

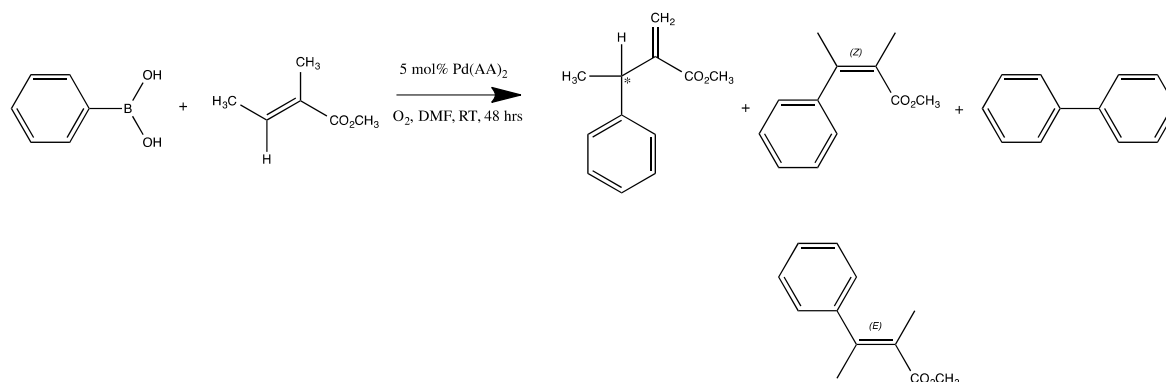


Figure 13. Bis(amino acid)Pd(II) catalyzed cross-coupling of phenylboronic acid and methyl tiglate.

2.3. Oxidative Coupling of Phenylboronic Acids and Alkenes

The standard coupling reaction that was used to evaluate the catalytic potential for each of the catalyst complexes was the aforementioned methyl tiglate and phenylboronic acid coupling [29,30]. This substrate was chosen because of the literature references already available to allow for comparison. All of the complexes described in this paper, except the N-methylproline complex, catalyzed this reaction and those data are summarized in Table 1 below. We have previously postulated that only the cis complexes are catalytically active, based on our observations with the glycine complexes described in a previous paper [67]. We see here, however, that the azetidine complex catalyzes the reaction even though it exists as the trans isomer. This suggests that N-alkylation, and not cis/trans geometry, may be the limiting factor in the catalytic ability of these complexes.

Table 1. Coupling reaction product distributions for catalysts **1**, **2**, **3**, **4**, **5**, **6**, **7**.

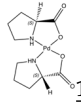
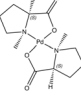
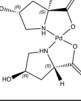
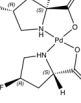
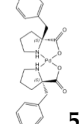
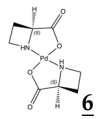
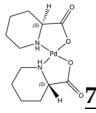
Complex	R/S Yield, %	% ee	E/Z Yield, %	Biaryl, %
 1	42	24	28	30
 2	No Reaction Observed			
 3	91	14	9	0
 4	94	11	6	0
 5	33	2	67	0

Table 1. Cont.

Complex	R/S Yield, %	% ee	E/Z Yield, %	Biaryl, %
	66	11	30	4
	97	1	2	1

Some general observations regarding product distributions and catalyst structure can be made based on our results. The presence of an electronegative group, –F or –OH, on the proline ring leads to a decrease in the formation of the E/Z products. The presence of purely alkyl functionality on the proline ring leads to an increase of the E/Z yield with corresponding loss of R/S product. The exception here is with the pipercolinic acid complex. This complex generates almost all R/S product, albeit with no enantioselectivity, and very little E/Z or homocoupled product. These general observations notwithstanding, there is still a great deal of variability in the product distributions that does not seem to follow any general trend. This suggests that the particular steric environment about the metal center during the catalytic cycle likely plays an important role in determining which products will form. As is often the case in examining various ligands for catalysis, it is difficult to separate the interplay between steric and electronic effects.

2.4. Proposed Mechanism of Pd-AA₂ Oxidative Coupling

The following mechanism is proposed for the palladium(II)-amino acid complex catalyzed oxidative coupling of phenylboronic acids to olefins (Figure 14, below). Step 1 involves the transmetalation of phenylboronic acid onto the palladium center. This is accomplished by an associative mechanism whereby the carboxylate group of one of the ligands de-coordinates to maintain a four-coordinate intermediate. The now-free carboxylate acts as a base towards the free boronic acid group, thus no addition of a base is required as is seen in a typical Suzuki coupling. The lack of catalytic activity of complex **2**, the N-methylated version of L-proline, shows the importance of the N-H bond for activity and the proposed mechanism suggests that H-bonding to a substrate is needed in this cycle.

DFT calculations show that the transmetalated intermediate has a geometry such that the metal center is completely occluded with the exception of a lobe of the empty d_z^2 orbital that lies above the palladium atom (Figure 15).

The dissociated carboxylate end of the aminoacidato ligand wraps under the metal and covers the other d_z^2 lobe. The remaining empty d_z^2 lobe is then free to coordinate a neutral olefin, maintaining charge neutrality. Insertion of the phenyl group into the olefin double bond, followed by β -hydride elimination, yields the observed products. There are two possible pathways for beta-hydride elimination. Hydride elimination from the methyl carbon yields the R/S product, while hydride elimination from the methine carbon yields the E/Z product. To regenerate the catalyst and begin the cycle again, molecular oxygen abstracts the hydride, generating a peroxide. Qualitative peroxide test strips do indicate the presence of minute quantities of peroxide in the 0–25 ppm range.

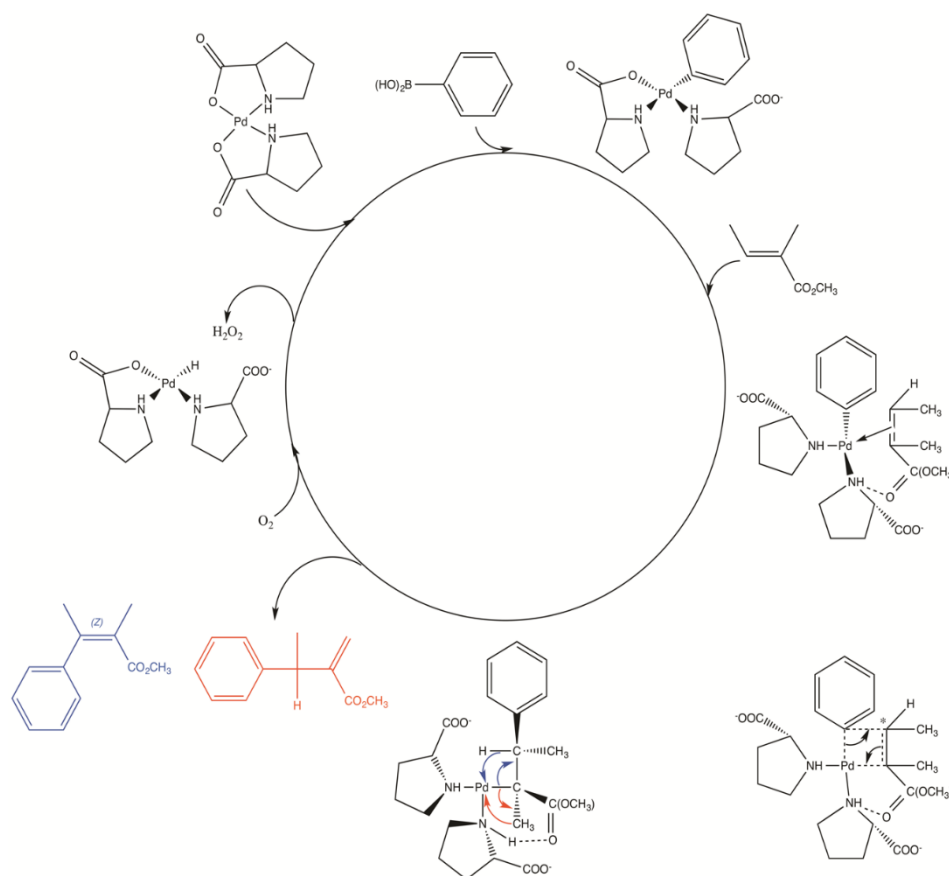


Figure 14. Proposed mechanism of the palladium(II)-amino acid complex catalyzed oxidative coupling of phenylboronic acids to olefins.

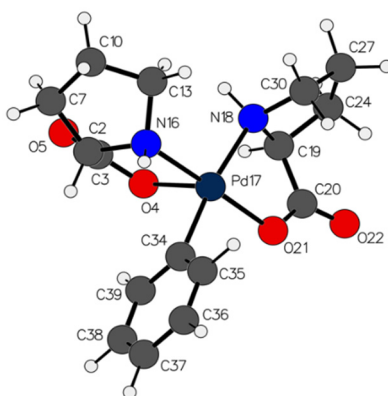


Figure 15. DFT-optimized geometry of the transmetalated intermediate. The non-occluded lobe of the d_z^2 orbital projects out of the page towards the reader.

2.5. Biaryl Formation

Biaryl formation results from the coupling of two phenyl boronic acid substrates. Biaryl formation was noted to occur for every catalyst; however, the degree of biaryl formation varied greatly. Steric considerations about the metal center must therefore allow for both of these groups to orient themselves cis to each other. The mechanism proposed above can be slightly modified to allow for this possibility. If we consider a second transmetalation step to occur rather than olefin coordination, the two phenyl groups are oriented cis to each other. Elimination of the biaryl yields a Pd^0 center, which is then oxidized by molecular oxygen back to a Pd^{II} center. It is not clear which factors may dampen biaryl

formation, but all of the substituted L-proline complexes as well as the piccolinate and azetidine showed little to no biaryl formation, a useful feature for an atom-economic process.

2.6. Multiple Insertions

A unique aspect of this coupling/catalyst system is the ability for the products to undergo additional coupling cycles. The initial alkene products of the coupling reaction can in turn enter the catalytic cycle again and undergo an additional phenylboronic acid addition. This second product can also re-enter the cycle for a third phenylboronic acid addition. We have observed one, two, and three phenylboronic acid addition products for these catalyst systems; however, a fourth addition product has not been observed for any catalyst. This is likely due to steric concerns whereby the third coupling product is simply too bulky to coordinate to the metal center. Given that the initial reaction conditions begin with a 3:1 excess of alkene to phenylboronic acid, noting products from multiple additions is particularly fascinating and suggests that the product of the first addition is activated toward further additions, a finding that will be the focus of a future study. In order to maximize additional couplings, the ratio was reversed to be 3:1 excess of phenylboronic acid to methyl tiglate. In the GC-MS of these coupling reactions, we observe three peaks of mass 190.2, six peaks of mass 266.3, and two peaks of mass 342.4; the fourth coupling product would have a mass of 418.5 if formed (Figure 16). For the actual chromatograms, see the Supplementary Materials.

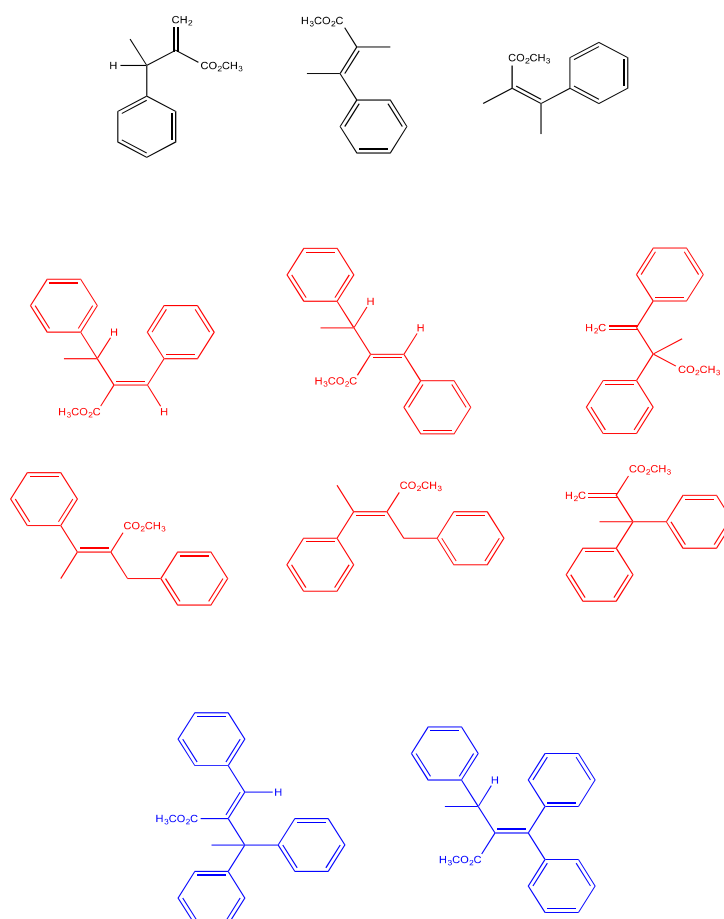


Figure 16. Postulated structures of multiple phenylboronic acid additions to the products of the bis(amino acid)Pd(II) catalyzed coupling of phenylboronic acid and methyl tiglate. First addition = black, second addition = red, third addition = blue.

2.7. Temperature Effects

Temperature has a significant effect on the enantioselectivity of the coupling reaction. The coupling reaction was carried out with the standard set of reaction conditions using the bis-proline complex as the catalyst at temperatures of 0, 25, and 65 °C. Enantioselectivities were noted to increase significantly with decreasing temperature as shown in Table 2, below. The equipment available for this study did not allow the reaction to be carried out below 0 °C and this could be an interesting study for the future with the proper equipment.

Table 2. Enantioselectivity versus temperature for the bis(amino acid)palladium(II) catalyzed oxidative coupling of phenylboronic acid to methyl tiglate.

Reaction Temperature, °C	%ee
65	~1
25	20
0	41

2.8. Solvent Effects

The standard coupling reaction was carried out in *N,N*-dimethylformamide, toluene, dichloromethane, and water solvents using the bis-proline complex as the catalyst. By far, DMF proved to be the superior solvent for this system. As a polar aprotic solvent, DMF has a hydrogen bond acceptor that greatly facilitates dissolution of the catalyst, which has unusually poor solubility in most common solvents. Subsequent trials were made with DMSO and acetonitrile as the solvents, but neither of these solvents gave appreciable product formation. As coordinating solvents, it is highly likely that solvent coordination to the complex blocks the active sites on the metal center required for reactivity. DMF, as a poorly-coordinating solvent, does not suffer this effect. No reaction was noted for either the dichloromethane (DCM) or toluene systems. DCM is a slightly polar aprotic solvent but lacks a hydrogen bond acceptor/donor, and toluene is a non-polar solvent. Neither of these solvents were observed to dissolve the catalyst, therefore the lack of any observed reactivity is not surprising. Water proved to be an interesting solvent choice. The catalyst is soluble in water, as is the phenylboronic acid substrate, but biphenyl formation was noted as the only reaction product. Methyl tiglate is extremely water-insoluble and the lack of PBA-MT cross-coupling products can be attributed to the lack of alkene solubility in water. This suggests that water may indeed be a “green” solvent choice for these systems so long as appropriate water-soluble substrates can be identified. Water as a solvent was used successfully for biaryl formation with a Pd(II) proline complex [78].

2.9. Pd(II)-Amino Acid Complexes as Polymerization Catalysts

Given the observation that these catalysts facilitate multiple substrate additions, it was hoped that they might also serve as novel polymerization catalysts. A suitable monomer containing both alkene and phenylboronic acid moieties, 4-(*trans*-3-methoxy-3-oxo-1-propen-1-yl)benzene boronic acid, was identified (Figure 17) and obtained for study.

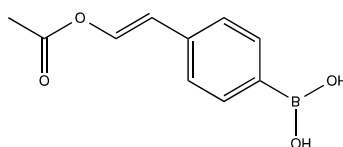


Figure 17. 4-(*trans*-3-methoxy-3-oxo-1-propen-1-yl)benzene boronic acid monomer.

The polymerization reaction was performed under conditions identical to the normal phenylboronic acid-methyl tiglate coupling using the *cis*-bis-(*L*-pipecolinato)palladium(II) complex as

the catalyst. This complex was chosen due to the fact that it exhibited the least amount of homocoupling. While high molecular weight polymer was not isolated from the reaction, high-resolution time-of-flight mass spectrometric analysis of the reaction provides evidence of oligomer formation. Mass spectral peaks corresponding to oligomer masses where $n = 2, 3, 4, 5,$ and 6 were observed ($n =$ number of monomeric repeat units) (Figure 18). The *cis*-bis-(L-pipecolinato)palladium(II) catalyst once again showed no formation of homocoupled monomer.



Figure 18. Proposed oligomer structures corresponding to HR-TOF MS data. From top left, $n = 2, 3, 4,$ 5, and 6 where $n =$ number of monomer units in the oligomer.

2.10. Other Coupling Substrates

There are hundreds, if not thousands, of possible boronic acid/olefin combinations that could be studied with our palladium(II)-amino acid catalytic systems. In an effort to probe some of the other possibilities of these systems, several substituted phenyl boronic acids and olefins were also examined as substrates for the coupling reaction.

An electron-withdrawing group on the phenyl boronic acid was introduced in the form of the trifluoromethyl group in 4-(trifluoromethyl)phenylboronic acid. The coupling reaction between this boronic acid and methyl tiglate was carried out as before with the bis-(L-prolinato)palladium(II) catalyst. The reaction proceeded smoothly with complete consumption of the phenylboronic acid substrate within the 48-hour reaction time. Product distributions were as follows: 71% R/S product with an enantiomeric excess of 11%, 24% homocoupled biaryl, 1% of the Z-alkene, and 4% of the secondary addition product (Figure 19).

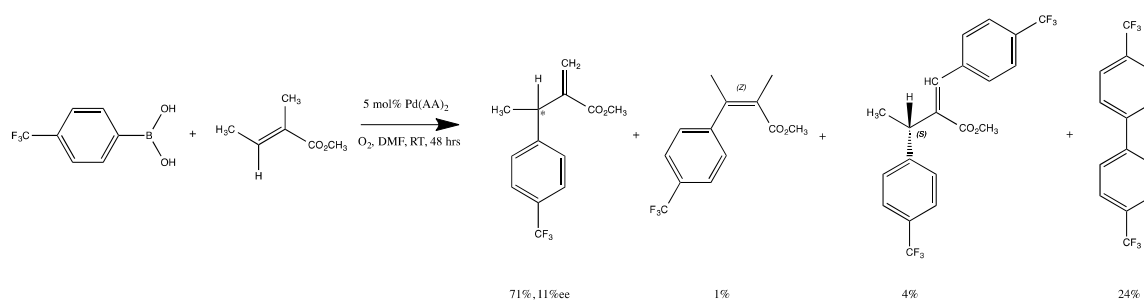


Figure 19. Reaction scheme and product distributions of the coupling reaction between 4-(trifluoromethyl)phenylboronic acid and methyl tiglate.

The same coupling reaction was also carried out with a phenylboronic acid with an electron donating group in the para position. In this case 4-methoxyphenylboronic acid was used (Figure 20).

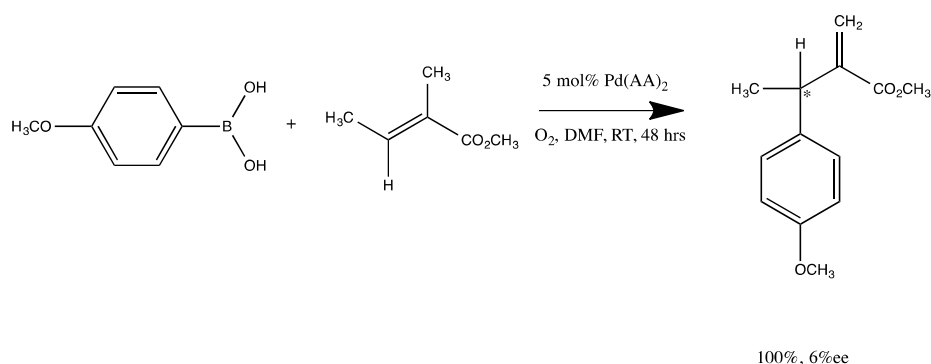


Figure 20. Reaction scheme and product distributions of the coupling reaction between 4-methoxyphenylboronic acid and methyl tiglate.

In this case, as before, complete consumption of the phenylboronic acid was observed. Interestingly, there was no evidence of homocoupling, alkene formation, or multiple phenylboronic acid additions noted for this reaction. The only product detected was the R/S product with an enantiomeric excess of 6%.

Methyl tiglate is considered to be an activated alkene, and it was hoped that our catalysts would also be useful for coupling non-activated alkenes. To this end *cis*-cyclooctene, 1,5-cyclooctadiene, and 1,5-hexadiene were evaluated with phenyl boronic acid in the standard coupling reaction. To our delight, all three alkenes coupled with phenylboronic acid when the reaction was catalyzed by the *cis*-bis-(L-prolinato)palladium(II) catalyst. The *cis*-cyclooctene coupling can generate four possible products (Figure 21), and four product peaks of the correct mass are observed in the GC-MS analysis of the reaction. The 1,5-cyclooctadiene coupling has two possible products (Figure 22), and here again we see two peaks of appropriate mass in the GC-MS trace. Finally, the 1,5-hexadiene coupling also has two possible products (Figure 23) and two peaks of correct mass are observed by GC-MS.

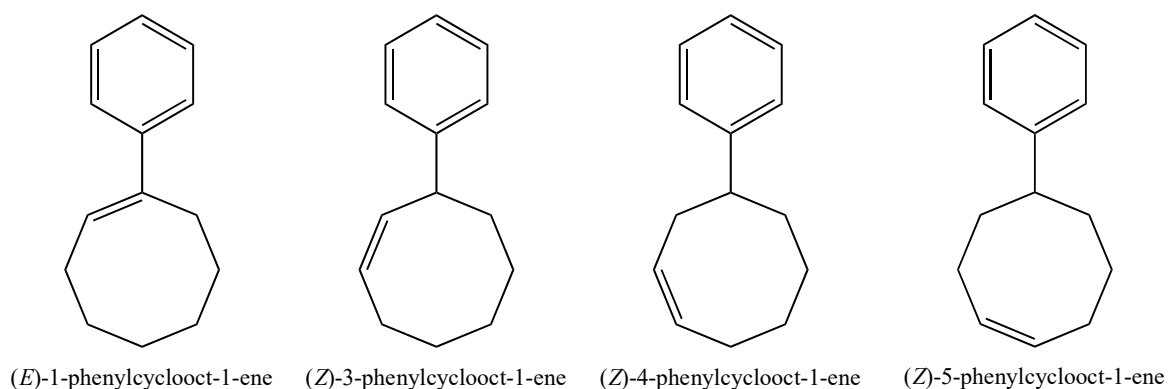


Figure 21. Possible product structures for the coupling reaction between phenylboronic acid and *cis*-cyclooctene.

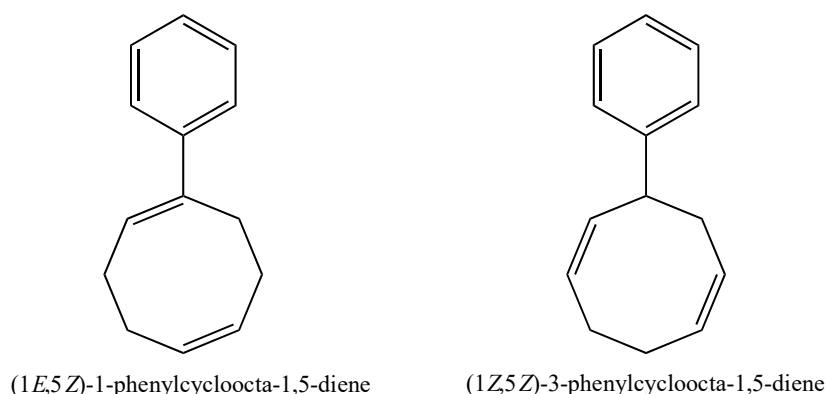


Figure 22. Possible product structures for the coupling reaction between phenylboronic acid and 1,5-cyclooctadiene.

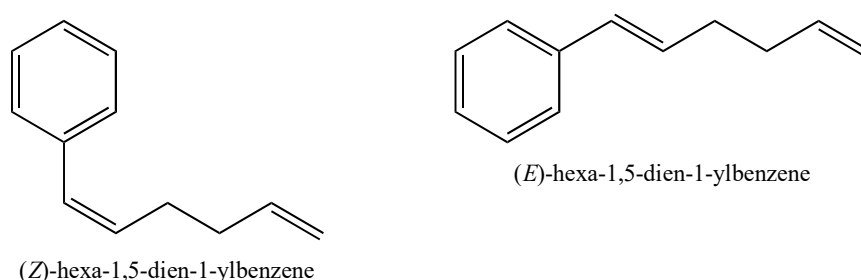


Figure 23. Possible product structures for the coupling reaction between phenylboronic acid and 1,5-hexadiene.

3. Materials and Methods

All reagents were purchased from commercial suppliers and used as received. Palladium(II) acetate was obtained from Pressure Chemical, Pittsburgh, PA, USA. Proline, N-methylproline, azetidine, and pipercolinic acid were purchased from Sigma-Aldrich, St. Louis, MO, USA. 4-fluoroproline, 4-hydroxyproline, and 2- α -benzylproline were purchased from Chem-Impex International, Inc., Wood Dale, IL, USA. Reagent grade solvents (ether, acetone, ethyl acetate, DMF) were purchased from Sigma-Aldrich. Deuterated solvents for NMR spectroscopy were obtained from Cambridge Isotope Laboratories, Tewksbury, MA, USA.

^1H and ^{13}C NMR spectra were collected on either a Varian MR-400 or a Bruker Avance III 600 MHz NMR spectrometer. High-Resolution Mass Spectra (HRMS) were collected on an Agilent 6220 (Santa Clara, CA, USA). Accurate Mass TOF LC-MS. X-ray crystallographic data were collected at 100 K on an Oxford Diffraction Gemini diffractometer with an EOS CCD detector and Mo $K\alpha$ radiation. Data collection and data reduction were performed using Agilent's CrysAlisPro software (Yarnton, Oxfordshire, UK) [79]. Structure solution and refinement were performed with ShelX [80,81], and Olex2 was used for graphical representation of the data [82].

All molecular modeling calculations were performed using Gaussian 09[83] using the WebMO interface. Full geometry optimizations and single-point energy calculations of all structures in water were performed via density functional theory (DFT) with the Becke three-parameter exchange functional [84] and the Lee–Yang–Parr correlation functional [85,86]. Because palladium is not covered in the cc-pVDZ basis set used, computations involving Pd employed Stuttgart/Dresden quasi-relativistic pseudopotentials [87].

3.1. General Procedure for the Synthesis of Palladium(II) Amino Acid Complexes

All reactions proceeded in very much identical ways and the following is the general procedure for all synthesis: An appropriately sized vial was fitted with a magnetic stir bar and charged with

palladium(II) acetate and an appropriate volume of 50/50 (*v/v*) acetone/water. The mixture was stirred until all solids had dissolved. To this we added the amino acid and stirred the mixture overnight. The reaction solutions turned from a clear red-orange to a clear pale-yellow supernatant with a pale-yellow precipitate. The supernatant was transferred via pipette to a clean vial and allowed to evaporate to give clear yellow needles. The pale-yellow precipitate was washed with water and dried under a vacuum. The combined yield of single crystals and precipitate was measured and the resulting solid was characterized by ^1H , ^{13}C , HRMS, C,H analysis, and single-crystal X-ray diffractometry where possible.

3.2. Synthesis of *cis-bis-(L-prolinato)palladium(II)* (1)

Following the general procedure, the following amounts were used: 55.7 mg palladium(II) acetate (0.2481 mmol), 3.0 mL of 50/50 (*v/v*) acetone/water and 57.1 mg L-proline (0.4960 mmol). Yield: 79.3 mg of product (0.2369 mmol, 96% yield). *Cis*-Pd(C₅H₈NO₂)₂ (**1**) was identified on the basis of the following data: ^1H NMR (400 MHz, D₂O) δ 4.08–3.63 (m, 1H), 3.37–2.73 (m, 2H), 2.28–1.52 (m, 4H). ^{13}C NMR (101 MHz, D₂O) δ 186.49, 64.89, 52.58, 29.31, 24.68. HRMS/ESI+ (*m/z*): [M+H]⁺ calcd for Pd(C₅H₈NO₂)₂, 335.0218; found, 335.0224. Anal. Calcd. for Pd(C₅H₈NO₂)₂: C, 35.89%; H, 4.82%; N, 8.37%. Found: C, 35.98%; H, 4.83%; N, 8.35%. X-ray crystallographic data -CCDC: 1913626.

3.3. Synthesis of *trans-bis-(N-methyl-L-prolinato)palladium(II)* (2)

Following the general procedure, the following amounts were used: 35.2 mg palladium(II) acetate (0.1568 mmol), 3.0 mL of 50/50 (*v/v*) acetone/water and *N*-methyl-L-proline (42.7 mg, 0.3306 mmol). Yield: 53.6 mg of product (0.1477 mmol, 94% yield). *Trans*-Pd(C₆H₁₀NO₂)₂ (**2**) was identified on the basis of the following data: ^1H NMR (400 MHz, D₂O) δ 3.28 (dd, *J* = 10.4, 7.0 Hz, 1H), 3.12 (ddd, *J* = 10.9, 7.0, 2.8 Hz, 1H), 2.71 (s, 3H), 2.61–2.47 (m, 1H), 2.42–2.13 (m, 3H), 1.99 (dtt, *J* = 12.9, 6.7, 3.4 Hz, 1H). HRMS/ESI+ (*m/z*): [M+H]⁺ calcd for Pd(C₆H₁₀NO₂)₂, 363.0531; found, 363.0532. Anal. Calcd. for Pd(C₆H₁₀NO₂)₂·2H₂O: C, 36.15%; H, 6.07%; N, 7.03%. Found: C, 37.61%; H, 5.85%; N, 7.29%. X-ray crystallographic data -CCDC: 1913622.

3.4. Synthesis of *cis-bis-(trans-4-hydrox-L-prolinato)palladium(II)* (3)

Following the general procedure, the following amounts were used: 59.4 mg palladium(II) acetate (0.2646 mmol), 2.0 mL of 50/50 (*v/v*) acetone/water and 77.1 mg 4-hydroxy-L-proline (0.5880 mmol). Yield: 94.3 mg of product (0.2572 mmol, 97% yield). *Cis*-Pd(C₅H₈NO₃)₂ (**3**) was identified on the basis of the following data: ^1H NMR (400 MHz, D₂O) δ 4.41 (s, 1H), 4.10 (t, *J* = 9.1 Hz, 1H), 3.35–3.28 (m, 1H), 3.27–3.15 (m, 2H), 3.10 (d, *J* = 12.7 Hz, 1H), 2.22–2.06 (m, 2H). HRMS/ESI+ (*m/z*): [M+H]⁺ calcd for Pd(C₅H₈NO₃)₂, 367.0116; found, 367.0130. Anal. Calcd. for Pd(C₅H₈NO₃)₂: C, 32.76%; H, 4.40%. Found: C, 32.88%; H, 4.42%. X-ray crystallographic data -CCDC: 1913624.

3.5. Synthesis of *cis-bis-(trans-4-fluoro-L-prolinato)palladium(II)* (4)

Following the general procedure, the following amounts were used: 49.6 mg palladium(II) acetate (0.2209 mmol), 3.0 mL of acetone and 64.6 mg *trans*-4-fluoro-L-proline (0.4853 mmol). Yield: 78.1 mg of product (0.2107 mmol, 95% yield). *Cis*-Pd(C₅H₇FNO₂)₂ (**4**) was identified on the basis of the following data: ^1H NMR (400 MHz, D₂O) δ 5.26–5.09 (m, 1H), 4.16–4.00 (m, 1H), 3.45–3.14 (m, 2H), 2.54–1.89 (m, 3H). ^{13}C NMR (101 MHz, D₂O) δ 186.09 (d, *J* = 140.5 Hz), 92.48 (d, *J* = 174.5 Hz), 62.48 (d, *J* = 150.3 Hz), 56.87 (dd, *J* = 131.2, 21.7 Hz), 36.10 (dd, *J* = 28.7, 21.6 Hz). ^{19}F NMR (471 MHz, D₂O) δ -179.33 (d, *J* = 140.9 Hz). HRMS/ESI+ (*m/z*): [M+H]⁺ calcd for Pd(C₅H₇FNO₂)₂, 371.0029; found, 371.0036. Anal. Calcd. for Pd(C₅H₇FNO₂)₂: C, 32.41%; H, 3.81%; N, 7.56%. Found: C, 32.99%; H, 3.92%; N, 7.53%. X-ray crystallographic data -CCDC: 1913621.

3.6. Synthesis of *trans*-bis-(2-benzylprolinato)palladium(II) (5)

Following the general procedure, the following amounts were used: 21.2 mg palladium(II) acetate (0.0944 mmol), 3.0 mL of 50/50 (*v/v*) acetone/water and 50.2 mg 2-benzylproline hydrochloride (0.2077 mmol). Yield: 44.7 mg of product (0.0868 mmol, 92% yield). *Trans*-Pd(C₁₂H₁₄NO₂)₂ (**5**) was identified on the basis of the following data: ¹H NMR (400 MHz, D₂O) δ 7.32–7.15 (m, 5H), 3.42 (d, *J* = 14.6 Hz, 1H), 3.36–3.23 (m, 2H), 3.00 (d, *J* = 14.6 Hz, 1H), 2.48–2.37 (m, 1H), 2.09–1.96 (m, 2H), 1.87 (pd, *J* = 9.7, 8.8, 3.6 Hz, 1H). HRMS/ESI+ (*m/z*): [M+H]⁺ calcd for Pd(C₁₂H₁₄NO₂)₂, 515.1157; found, 515.1175. Anal. Calcd. for Pd(C₁₂H₁₄NO₂)₂: C, 55.98%; H, 5.48%; N, 5.44%. Found: C, 55.95%; H, 5.52%; N, 5.37%. X-ray crystallographic data -CCDC: 1913619.

3.7. Synthesis of *trans*-bis-(L-azetidine-2-carboxylato)palladium(II) (6)

Following the general procedure, the following amounts were used: 49.9 mg palladium(II) acetate (0.2223 mmol), 2.0 mL of 50/50 (*v/v*) acetone/water and 51.2 mg L-azetidine-2-carboxylic acid (0.5064 mmol). Yield: 66.7 mg of product (0.2175 mmol, 98% yield). *Trans*-Pd(C₄H₆NO₂)₂ (**6**) was identified on the basis of the following data: ¹H NMR (400 MHz, D₂O) δ 4.44 (dt, *J* = 17.3, 8.8 Hz, 1H), 3.75–3.64 (m, 2H), 2.81–2.68 (m, 1H), 2.67–2.55 (m, 2H). ¹³C NMR (101 MHz, D₂O) δ 187.86, 186.59, 63.36, 61.42, 50.32, 48.79, 24.61, 24.58. HRMS/ESI+ (*m/z*): [M+H]⁺ calcd for Pd(C₄H₆NO₂)₂, 515.1157; found, 515.1175. Anal. Calcd. for Pd(C₄H₆NO₂)₂: C, 55.98%; H, 5.48%; N, 5.44%. Found: C, 55.95%; H, 5.52%; N, 5.37%.

3.8. Synthesis of *cis*-bis-(L-pipecolinato)palladium(II) (7)

Following the general procedure, the following amounts were used: 107.5 mg palladium(II) acetate (0.4788 mmol), 3.0 mL of 50/50 (*v/v*) acetone/water, and 126.6 mg L-pipecolinic acid (0.9802 mmol). Yield: 152.4 mg of product (0.4202 mmol, 88% yield). *Cis*-Pd(C₆H₁₀NO₂)₂ (**7**) was identified on the basis of the following data: ¹H NMR (400 MHz, D₂O) δ 3.78–3.57 (m, 1H), 2.96–2.63 (m, 2H), 1.94–1.08 (m, 6H). HRMS/ESI+ (*m/z*): [M+H]⁺ calcd for Pd(C₆H₁₀NO₂)₂, 363.0531; found, 363.0543. Anal. Calcd. for Pd(C₆H₁₀NO₂)₂·4H₂O: C, 33.15%; H, 6.49%; N, 6.44%. Found: C, 33.30%; H, 6.50%; N, 6.45%. X-ray crystallographic data -CCDC: 1913623.

3.9. Synthesis of *cis*-bis-(D-prolinato)palladium(II) (8)

Following the general procedure, the following amounts were used: 50.2 mg palladium(II) acetate (0.2236 mmol), 2.0 mL of 50/50 (*v/v*) acetone/water, and 58.7 mg D-proline (0.5099 mmol). Yield: 71.1 mg of product (0.2124 mmol, 95% yield). *Cis*-Pd(C₅H₈NO₂)₂ (**8**) was identified on the basis of the following data: ¹H NMR (400 MHz, D₂O) δ 3.79 (dd, *J* = 9.1, 7.6 Hz, 1H), 3.10–2.96 (m, 2H), 2.17–2.06 (m, 1H), 1.99–1.78 (m, 2H), 1.67–1.54 (m, 1H). HRMS/ESI+ (*m/z*): [M+H]⁺ calcd for Pd(C₅H₈NO₂)₂, 335.0218; found, 335.0222. Anal. Calcd. for Pd(C₅H₈NO₂)₂: C, 35.89%; H, 4.82%; N, 8.37%. Found: C, 36.10%; H, 4.72%; N, 8.45%. X-ray crystallographic data -CCDC: 1913620.

3.10. Synthesis of *cis*-bis-(D-pipecolinato)palladium(II) (9)

Following the general procedure, the following amounts were used: 112.8 mg palladium(II) acetate (0.5024 mmol), 2.0 mL of 50/50 (*v/v*) acetone/water and 132.2 mg D-pipecolinic acid (1.0235 mmol). Yield: 151.9 mg of product (0.4188 mmol, 83% yield). *Cis*-Pd(C₆H₁₀NO₂)₂ (**9**) was identified on the basis of the following data: ¹H NMR (400 MHz, D₂O) δ 3.75–3.56 (m, 1H), 2.97–2.66 (m, 2H), 2.08–1.08 (m, 6H). HRMS/ESI+ (*m/z*): [M+H]⁺ calcd for Pd(C₆H₁₀NO₂)₂, 363.0531; found, 363.0520. Anal. Calcd. for Pd(C₆H₁₀NO₂)₂·4H₂O: C, 33.15%; H, 6.49%; N, 6.44%. Found: C, 35.09%; H, 6.02%; N, 6.85%. X-ray crystallographic data -CCDC: 1913625.

3.11. General Procedure for Catalytic Reactions

The couplings were carried out in DMF solvent under an O₂ atmosphere with a 3:1 alkene:boronic acid ratio and 5 mol % catalyst loading, based on the boronic acid. Coupling reactions were stirred under O₂ for 48 h. The reaction work-up consisted of dilution with water followed by extraction with ethyl acetate and drying over anhydrous magnesium sulfate. Analysis included chiral GC using an Agilent CP-ChiralSil-Dex CB column (Agilent Technologies, Santa Clara, CA, USA).

In order to better analyze the multiple coupling products, the methyl tiglate to boronic acid ratio was changed to make the alkene:boronic acid ratio 1:3.

4. Conclusions

Nine palladium(II) bis-amino acid chelates with aliphatic ring structures for their R-group have been synthesized, characterized, and tested for catalytic activity for the oxidative coupling of phenylboronic acid with olefins. The amino acids employed include L-proline, D-proline, N-methylproline, azetidine, L-pipecolinic acid, D-pipecolinic acid, 2- α -benzylproline, 4-hydroxyproline, and 4-fluoroproline. The N-methylproline, 2- α -benzylproline, and azetidine complexes exist as the *trans* isomer, with all other complexes being *cis*. All of these complexes are square planar, C₂ symmetric molecules that exhibit varying degrees of intermolecular hydrogen bonding. All complexes are catalytically active with respect to the oxidative coupling of phenylboronic acids to olefins, with the exception of the N-methylproline complex. Enantioselectivities are modest with the best example, *cis*-bis(prolinato)palladium(II), yielding an enantiomeric excess of 24% with enantioselectivity increasing with decreasing temperature. These complexes couple a wide variety of both electron-rich and electron-deficient phenylboronic acids and activated and non-activated olefins. The finding of multiple cross-couplings on a single substrate is a fascinating finding that will be the subject of future studies.

Supplementary Materials: The following are available online at <http://www.mdpi.com/2073-4344/9/6/515/s1>, Figure S1: Example of mass spectrum showing Pd isotope pattern, Figure S2. Packing diagram for Complex 3 showing hydrogen-bonding motif; Figure S3. Packing diagram for Complex 4 showing hydrogen-bonding motif; Figure S4. Packing diagram for Complex 5 showing hydrogen-bonding motif. Figure S5. Packing diagram for Complex 7 showing hydrogen-bonding motif; Figure S6. Typical GC-MS trace of the first oxidative coupling of phenylboronic acid with methyl tiglate; Figure S7. Typical GC-MS trace of the second oxidative coupling products of phenylboronic acid with methyl tiglate; Figure S8. Typical GC-MS trace of the Third oxidative coupling products of phenylboronic acid with methyl tiglate; Report I. Complete crystallographic experimental parameters and tables of bond lengths and angles for complex 1. Report II. Complete crystallographic experimental parameters and tables of bond lengths and angles for complex 2. Report III. Complete crystallographic experimental parameters and tables of bond lengths and angles for complex 3. Report IV. Complete crystallographic experimental parameters and tables of bond lengths and angles for complex 4. Report V. Complete crystallographic experimental parameters and tables of bond lengths and angles for complex 5. Report VI. Complete crystallographic experimental parameters and tables of bond lengths and angles for complex 6. Report VII. Complete crystallographic experimental parameters and tables of bond lengths and angles for complex 8. Report VIII. Complete crystallographic experimental parameters and tables of bond lengths and angles for complex 9. Example of HRMS showing Pd isotope pattern, figures showing crystal lattice hydrogen-bonding motifs for select complexes, GC-MS traces showing the multiple cross-coupling analysis and full experimental data and complete listing of bond lengths and angles for compounds 1-9. In addition, CCDC numbers 1913619-1913626 contain the full supplementary .cif files for this paper. These data can be obtained free of charge from the Cambridge Crystallographic Data Centre via www.ccdc.cam.ac.uk/structures.

Author Contributions: Conceptualization, J.S.M. and D.B.H.J. Synthesis and characterization of compounds, D.B.H.J., H.M.R., S.S., J.M., and J.W.M.

Funding: This research received funding in the form of a \$1000 grant for syringes from the Hamilton Syringe Company. The authors gratefully acknowledge the Virginia Tech Open Access Subvention Fund for funding the open access fee for this article.

Conflicts of Interest: The authors declare no conflict of interest.

References

1. Jin, L.Q.; Lei, A.W. Mechanistic aspects of oxidation of palladium with O₂. *Sci. China Chem.* **2012**, *55*, 2027–2035. [[CrossRef](#)]
2. Beccalli, E.M.; Broggin, G.; Martinelli, M.; Sottocornola, S. C-C, C-O, C-N Bond Formation on sp² Carbon by Palladium(II)-Catalyzed Reactions Involving Oxidant Agents. *Chem. Rev.* **2007**, *107*, 5318–5365. [[CrossRef](#)]
3. Obora, Y.; Ishii, Y. Pd(II)/HPMoV-catalyzed direct oxidative coupling reaction of benzene derivatives with olefins. *Molecules* **2010**, *15*, 1487–1500. [[CrossRef](#)] [[PubMed](#)]
4. Stahl, S.S. Palladium oxidase catalysis. Selective oxidation of organic chemicals by direct dioxygen-coupled turnover. *Angew. Chem. Int. Ed.* **2004**, *43*, 3400–3420. [[CrossRef](#)] [[PubMed](#)]
5. Wu, W.; Jiang, H. Palladium-Catalyzed Oxidation of Unsaturated Hydrocarbons Using Molecular Oxygen. *Acc. Chem. Res.* **2012**, *45*, 1736–1748. [[CrossRef](#)] [[PubMed](#)]
6. Zeni, G.; Larock, R.C. Synthesis of heterocycles via palladium-catalyzed oxidative addition. *Chem. Rev.* **2006**, *106*, 4644–4680. [[CrossRef](#)] [[PubMed](#)]
7. Lu, Y.; Goldstein, E.L.; Stoltz, B.M. Palladium-Catalyzed Enantioselective Csp³-Csp³ Cross-Coupling for the Synthesis of (Poly)fluorinated Chiral Building Blocks. *Org. Lett.* **2018**, *20*, 5657–5660. [[CrossRef](#)] [[PubMed](#)]
8. Khan, F.; Dlugosch, M.; Liu, X.; Banwell, M.G. The Palladium-Catalyzed Ullmann Cross-Coupling Reaction: A Modern Variant on a Time-Honored Process. *Acc. Chem. Res.* **2018**, *51*, 1784–1795. [[CrossRef](#)] [[PubMed](#)]
9. Christoffel, F.; Ward, T.R. Palladium-Catalyzed Heck Cross-Coupling Reactions in Water: A Comprehensive Review. *Catal. Lett.* **2018**, *148*, 489–511. [[CrossRef](#)]
10. Roy, D.; Uozumi, Y. Recent Advances in Palladium-Catalyzed Cross-Coupling Reactions at ppm to ppb Molar Catalyst Loadings. *Adv. Synth. Catal.* **2018**, *360*, 602–625. [[CrossRef](#)]
11. Biffis, A.; Centomo, P.; Del Zotto, A.; Zecca, M. Pd Metal Catalysts for Cross-Couplings and Related Reactions in the 21st Century: A Critical Review. *Chem. Rev.* **2018**, *118*, 2249–2295. [[CrossRef](#)] [[PubMed](#)]
12. Devendar, P.; Qu, R.Y.; Kang, W.M.; He, B.; Yang, G.F. Palladium-Catalyzed Cross-Coupling Reactions: A Powerful Tool for the Synthesis of Agrochemicals. *J. Agric. Food Chem.* **2018**, *66*, 8914–8934. [[CrossRef](#)] [[PubMed](#)]
13. Sherwood, J.; Clark, J.H.; Fairlamb, I.J.S.; Slattery, J.M. Solvent effects in palladium catalysed cross-coupling reactions. *Green Chem.* **2019**, *21*, 2164–2213. [[CrossRef](#)]
14. Gligorich, K.M.; Cummings, S.A.; Sigman, M.S. Palladium-catalyzed reductive coupling of styrenes and organostannanes under aerobic conditions. *J. Am. Chem. Soc.* **2007**, *129*, 14193–14195. [[CrossRef](#)] [[PubMed](#)]
15. Adamo, C.; Amatore, C.; Ciofini, I.; Jutand, A.; Lakmini, H. Mechanism of the Palladium-Catalyzed Homocoupling of Arylboronic Acids: Key Involvement of a Palladium Peroxo Complex. *J. Am. Chem. Soc.* **2006**, *128*, 6829–6836. [[CrossRef](#)]
16. Canovese, L.; Visentin, F.; Chessa, G.; Santo, C.; Levi, C.; Uguagliati, P. Oxidative coupling of activated alkynes with palladium(0) olefin complexes: Side production of the highly symmetric hexamethyl mellitate species under mild conditions at low alkyne/complex molar ratios. *Inorg. Chem. Commun.* **2006**, *9*, 388–390. [[CrossRef](#)]
17. Hull, K.L.; Lanni, E.L.; Sanford, M.S. Highly Regioselective Catalytic Oxidative Coupling Reactions: Synthetic and Mechanistic Investigations. *J. Am. Chem. Soc.* **2006**, *128*, 14047–14049. [[CrossRef](#)]
18. Hull, K.L.; Sanford, M.S. Determining the mechanism of palladium-catalyzed oxidative coupling reactions. In Proceedings of the 239th ACS National Meeting & Exposition, San Francisco, CA, USA, 21–25 March 2010.
19. Lu, Y.; Wang, D.-H.; Engle, K.M.; Yu, J.-Q. Pd(II)-Catalyzed Hydroxyl-Directed C-H Olefination Enabled by Monoprotected Amino Acid Ligands. *J. Am. Chem. Soc.* **2010**, *132*, 5916–5921. [[CrossRef](#)]
20. Muzart, J. Molecular oxygen to regenerate Pd(II) active species. *Chem. Asian J.* **2006**, *1*, 508–515. [[CrossRef](#)]
21. Lei, A.; Zhang, X. A novel palladium-catalyzed homocoupling reaction initiated by transmetalation of palladium enolates. *Tetrahedron Lett.* **2002**, *43*, 2525–2528. [[CrossRef](#)]
22. Liegault, B.; Fagnou, K. Palladium-Catalyzed Intramolecular Coupling of Arenes and Unactivated Alkanes in Air. *Organometallics* **2008**, *27*, 4841–4843. [[CrossRef](#)]
23. Liu, C.; Jin, L.; Lei, A. Transition-metal-catalyzed oxidative cross-coupling reactions. *Synlett* **2010**, *2010*, 2527–2536.

24. Martinez, C.; Alvarez, R.; Aurrecochea, J.M. Palladium-Catalyzed Sequential Oxidative Cyclization/Coupling of 2-Alkynylphenols and Alkenes: A Direct Entry into 3-Alkenylbenzofurans. *Org. Lett.* **2009**, *11*, 1083–1086. [[CrossRef](#)] [[PubMed](#)]
25. Prateptongkum, S.; Driller, K.M.; Jackstell, R.; Spannenberg, A.; Beller, M. Efficient Synthesis of Biologically Interesting 3,4-Diaryl-Substituted Succinimides and Maleimides: Application of Iron-Catalyzed Carbonylations. *Chem. Eur. J.* **2010**, *16*, 9606–9615. [[CrossRef](#)] [[PubMed](#)]
26. Van Aeken, S.; Verbeeck, S.; Deblander, J.; Maes, B.U.W.; Tehrani, K.A. Synthesis of 3-substituted benzo[*g*]isoquinoline-5,10-diones: A convenient one-pot Sonogashira coupling/iminoannulation procedure. *Tetrahedron* **2011**, *67*, 2269–2278. [[CrossRef](#)]
27. Venkatraman, S.; Huang, T.; Li, C.-J. Carbon-carbon bond formation via palladium-catalyzed reductive coupling of aryl halides in air and water. *Adv. Synth. Catal.* **2002**, *344*, 399–405. [[CrossRef](#)]
28. Wakioka, M.; Mutoh, Y.; Takita, R.; Ozawa, F. A highly selective catalytic system for the cross-coupling of (*E*)-styryl bromide with benzene boronic acid: Application to the synthesis of all-trans poly(arylenevinylene)s. *Bull. Chem. Soc. Jpn.* **2009**, *82*, 1292–1298. [[CrossRef](#)]
29. Yoo, K.S.; O'Neill, J.; Sakaguchi, S.; Giles, R.; Lee, J.H.; Jung, K.W. Asymmetric Intermolecular Boron Heck-Type Reactions via Oxidative Palladium(II) Catalysis with Chiral Tridentate NHC-Amidate-Alkoxide Ligands. *J. Org. Chem.* **2010**, *75*, 95–101. [[CrossRef](#)]
30. Yoo, K.S.; Park, C.P.; Yoon, C.H.; Sakaguchi, S.; O'Neill, J.; Jung, K.W. Asymmetric Intermolecular Heck-Type Reaction of Acyclic Alkenes via Oxidative Palladium(II) Catalysis. *Org. Lett.* **2007**, *9*, 3933–3935. [[CrossRef](#)]
31. Chen, Q.; Li, C. Activation of the Vinylic C-Cl Bond by Complexation of Fe(CO)₃: Palladium-Catalyzed Coupling Reactions of (η^4 -Chlorodiene)tricarbonyliron Complexes. *Organometallics* **2007**, *26*, 223–229. [[CrossRef](#)]
32. Yoo, K.S.; Yoon, C.H.; Jung, K.W. Oxidative Palladium(II) Catalysis: A Highly Efficient and Chemoselective Cross-Coupling Method for Carbon-Carbon Bond Formation under Base-Free and Nitrogenous-Ligand Conditions. *J. Am. Chem. Soc.* **2006**, *128*, 16384–16393. [[CrossRef](#)] [[PubMed](#)]
33. Heck, R.F.; Nolley, J., Jr. P. Palladium-catalyzed vinylic hydrogen substitution reactions with aryl, benzyl, and styryl halides. *J. Org. Chem.* **1972**, *37*, 2320–2322. [[CrossRef](#)]
34. Herr, R.J.; Dowling, M.S.; Scampini, A.C.; Smith, T.M. Iridium- and Palladium-Catalyzed Syntheses of (*S*)(+) and (*R*)(-) Coniine from Enantiopure Allylic Alcohols. In Proceedings of the 35th Northeast Regional Meeting of the American Chemical Society, Burlington, VT, USA, 29 June–2 July 2008.
35. Horiguchi, H.; Tsurugi, H.; Satoh, T.; Miura, M. Palladium/phosphite or phosphate catalyzed oxidative coupling of arylboronic acids with alkynes to produce 1,4-diaryl-1,3-butadienes. *Adv. Synth. Catal.* **2008**, *350*, 509–514. [[CrossRef](#)]
36. Jin, L.; Zhao, Y.; Wang, H.; Lei, A. Palladium-catalyzed R(sp³)-Zn/R(sp)-SnBu₃ oxidative cross-coupling. *Synthesis* **2008**, *2008*, 649–654.
37. Johnson, T.; Lautens, M. Palladium(II)-Catalyzed Enantioselective Synthesis of α -(Trifluoromethyl)arylmethylamines. *Org. Lett.* **2013**, *15*, 4043–4045. [[CrossRef](#)]
38. Jordan-Hore, J.A.; Sanderson, J.N.; Lee, A.-L. Mild and Ligand-Free Pd(II)-Catalyzed Conjugate Additions to Hindered γ -Substituted Cyclohexenones. *Org. Lett.* **2012**, *14*, 2508–2511. [[CrossRef](#)] [[PubMed](#)]
39. Khabibulin, V.R.; Kulik, A.V.; Oshanina, I.V.; Bruk, L.G.; Temkin, O.N.; Nosova, V.M.; Ustynyuk, Y.A.; Bel'skii, V.K.; Stash, A.I.; Lysenko, K.A.; et al. Mechanism of the Oxidative Carbonylation of Terminal Alkynes at the C-H Bond in Solutions of Palladium Complexes. *Kinet. Catal.* **2007**, *48*, 228–244. [[CrossRef](#)]
40. Alvarez, R.; Martinez, C.; Madich, Y.; Denis, J.G.; Aurrecochea Jose, M.; de Lera Angel, R. A general synthesis of alkenyl-substituted benzofurans, indoles, and isoquinolones by cascade palladium-catalyzed heterocyclization/oxidative Heck coupling. *Chemistry* **2010**, *16*, 12746–12753. [[CrossRef](#)]
41. Aouf, C.; Thierry, E.; Le Bras, J.; Muzart, J. Palladium-Catalyzed Dehydrogenative Coupling of Furans with Styrenes. *Org. Lett.* **2009**, *11*, 4096–4099. [[CrossRef](#)]
42. Beccalli, E.M.; Borsini, E.; Broggin, G.; Rigamonti, M.; Sottocornola, S. Intramolecular palladium-catalyzed oxidative coupling on thiophene and furan rings. Determinant role of the electronic availability of the heterocycle. *Synlett* **2008**, *2008*, 1053–1057.
43. Maehara, A.; Satoh, T.; Miura, M. Palladium-catalyzed direct oxidative vinylation of thiophenes and furans under weakly basic conditions. *Tetrahedron* **2008**, *64*, 5982–5986. [[CrossRef](#)]

44. Thiery, E.; Harakat, D.; Le Bras, J.; Muzart, J. Palladium-Catalyzed Oxidative Coupling of 2-Alkylfurans with Olefins through C-H Activation: Synthesis of Difurylalkanes. *Organometallics* **2008**, *27*, 3996–4004. [[CrossRef](#)]
45. Xi, P.; Yang, F.; Qin, S.; Zhao, D.; Lan, J.; Gao, G.; Hu, C.; You, J. Palladium(II)-Catalyzed Oxidative C-H/C-H Cross-Coupling of Heteroarenes. *J. Am. Chem. Soc.* **2010**, *132*, 1822–1824. [[CrossRef](#)] [[PubMed](#)]
46. Yamashita, M.; Hirano, K.; Satoh, T.; Miura, M. Synthesis of Condensed Heteroaromatic Compounds by Palladium-Catalyzed Oxidative Coupling of Heteroarene Carboxylic Acids with Alkynes. *Org. Lett.* **2009**, *11*, 2337–2340. [[CrossRef](#)] [[PubMed](#)]
47. Yang, S.-D.; Sun, C.-L.; Fang, Z.; Li, B.-J.; Li, Y.-Z.; Shi, Z.-J. Palladium-catalyzed direct arylation of (hetero)arenes with aryl boronic acids. *Angew. Chem. Int. Ed.* **2008**, *47*, 1473–1476. [[CrossRef](#)] [[PubMed](#)]
48. Bardhan, S.; Wacharasindhu, S.; Wan, Z.-K.; Mansour, T.S. Heteroaryl ethers by oxidative palladium catalysis of pyridotriazol-1-yloxy pyrimidines with arylboronic acids. *Org. Lett.* **2009**, *11*, 2511–2514. [[CrossRef](#)]
49. Belitsky, J.M. Palladium catalyzed homocoupling of indole and aryl boronic acids. In Proceedings of the 236th ACS National Meeting, Philadelphia, PA, USA, 17–21 August 2008.
50. Belitsky, J.M. Palladium Catalyzed Homocoupling of Indole and Aryl Boronic Acids. In Proceedings of the Abstract Central Cent. Regional Meeting of the American Chemical Society, Cleveland, OH, USA, 20–23 May 2009.
51. Clawson, R.W.; Deavers, R.E.; Akhmedov, N.G.; Soederberg, B.C.G. Palladium-catalyzed synthesis of 3-alkoxy-substituted indoles. *Tetrahedron* **2006**, *62*, 10829–10834. [[CrossRef](#)]
52. Djakovitch, L.; Rouge, P. New homogeneously and heterogeneously [Pd/Cu]-catalysed C3-alkenylation of free NH-indoles. *J. Mol. Catal. A Chem.* **2007**, *273*, 230–239. [[CrossRef](#)]
53. Gong, X.; Song, G.; Zhang, H.; Li, X. Palladium-Catalyzed Oxidative Cross-Coupling between Pyridine N-Oxides and Indoles. *Org. Lett.* **2011**, *13*, 1766–1769. [[CrossRef](#)]
54. He, C.-Y.; Fan, S.; Zhang, X. Pd-catalyzed oxidative cross-coupling of perfluoroarenes with aromatic heterocycles. *J. Am. Chem. Soc.* **2010**, *132*, 12850–12852. [[CrossRef](#)]
55. Wang, Z.; Li, K.; Zhao, D.; Lan, J.; You, J. Palladium-Catalyzed Oxidative C-H/C-H Cross-Coupling of Indoles and Pyrroles with Heteroarenes. *Angew. Chem. Int. Ed.* **2011**, *50*, 5365–5369. [[CrossRef](#)] [[PubMed](#)]
56. Henke, A.; Srogl, J. Pd²⁺ and Cu²⁺ catalyzed oxidative cross-coupling of mercaptoacetylenes and arylboronic acids. *Chem. Commun.* **2011**, *47*, 4282–4284. [[CrossRef](#)] [[PubMed](#)]
57. Kirchberg, S.; Tani, S.; Ueda, K.; Yamaguchi, J.; Studer, A.; Itami, K. Oxidative biaryl coupling of thiophenes and thiazoles with arylboronic acids through palladium catalysis: Otherwise difficult C4-selective C-H arylation enabled by boronic acids. *Angew. Chem. Int. Ed.* **2011**, *50*, 2387–2391. [[CrossRef](#)] [[PubMed](#)]
58. Schwan, A.L. Palladium catalyzed cross-coupling reactions for phosphorus-carbon bond formation. *Chem. Soc. Rev.* **2004**, *33*, 218–224. [[CrossRef](#)] [[PubMed](#)]
59. Wagner-Schuh, B.; Beck, W. Metal Complexes of Biologically Important Ligands, CLXXVII. Dichlorido Platinum(II) and Palladium(II) Complexes with Long Chain Amino Acids and Amino Acid Amides. *Z. Anorg. Allg. Chem.* **2017**, *643*, 632–635. [[CrossRef](#)]
60. Liu, R.R.; Li, B.L.; Lu, J.; Shen, C.; Gao, J.R.; Jia, Y.X. Palladium/l-Proline-Catalyzed Enantioselective α -Arylation Desymmetrization of Cyclohexanones. *J. Am. Chem. Soc.* **2016**, *138*, 5198–5201. [[CrossRef](#)]
61. Tselikhovskiy, D.; Popov, I.; Gutkin, V.; Rozin, A.; Shvartsman, A.; Blum, J. On the involvement of palladium nanoparticles in the Heck and Suzuki reactions. *European J. Org. Chem.* **2009**, 98–102. [[CrossRef](#)]
62. Chatterjee, A.; Ward, T.R. Recent Advances in the Palladium Catalyzed Suzuki-Miyaura Cross-Coupling Reaction in Water. *Catal. Letters* **2016**, *146*, 820–840. [[CrossRef](#)]
63. Klaerner, C.; Greiner, A. Synthesis of polybenzyls by Suzuki Pd-catalyzed crosscoupling of boronic acids and benzyl bromides. Model reactions and polyreactions. *Macromol. Rapid Commun.* **1998**, *19*, 605–608. [[CrossRef](#)]
64. Wu, N.; Li, X.; Xu, X.; Wang, Y.; Xu, Y.; Chen, X. Homocoupling reaction of aryl boronic acids catalyzed by Pd(OAc)₂/K₂CO₃ in water under air atmosphere. *Lett. Org. Chem.* **2010**, *7*, 11–14. [[CrossRef](#)]
65. Xu, Z.; Mao, J.; Zhang, Y. Pd(OAc)₂-catalyzed room temperature homocoupling reaction of arylboronic acids under air without ligand. *Catal. Commun.* **2007**, *9*, 97–100. [[CrossRef](#)]
66. Yamamoto, Y. Homocoupling of arylboronic acids with a catalyst system consisting of a palladium(II) N-heterocyclic carbene complex and p-benzoquinone. *Synlett* **2007**, 1913–1916. [[CrossRef](#)]
67. Zhou, L.; Xu, Q.X.; Jiang, H.F. Palladium-catalyzed homo-coupling of boronic acids with supported reagents in supercritical carbon dioxide. *Chin. Chem. Lett.* **2007**, *18*, 1043–1046. [[CrossRef](#)]

68. Morris, D.M.D.M.; McGeagh, M.; De Peña, D.; Merola, J.S. Extending the range of pentasubstituted cyclopentadienyl compounds: The synthesis of a series of tetramethyl(alkyl or aryl)cyclopentadienes (Cp^{*R}), their iridium complexes and their catalytic activity for asymmetric transfer hydrogenation. *Polyhedron* **2014**, *84*, 120–135. [CrossRef]
69. Hobart, D.B.; Berg, M.A.G.G.; Merola, J.S. Bis-glycinato complexes of palladium(II): Synthesis, structural determination, and hydrogen bonding interactions. *Inorg. Chim. Acta* **2014**, *423*, 21–30. [CrossRef]
70. Ito, T.; Marumo, F.; Saito, Y. The crystal structure of bis-(L-prolinato)palladium(II). *Acta Crystallogr. Sect. B Struct. Crystallogr. Cryst. Chem.* **2002**, *27*, 1062–1066. [CrossRef]
71. Chernova, N.N.; Strukov, V.V.; Avetikyan, G.B.; Chernonozhkin, V.N. Synthesis and structure of complex palladium(II) bis(histidinate)s. *Zh. Neorg. Khim.* **1980**, *25*, 1569–1574.
72. Jarzab, T.C.; Hare, C.R.; Langs, D.A. cis-Bis(L-tyrosinato)palladium(II) hemihydrate, $C_{36}H_{42}N_4O_{13}Pd_2$. *Cryst. Struct. Commun.* **1973**, *2*, 399–403.
73. Jarzab, T.C.; Hare, C.R.; Langs, D.A. cis-Bis(L-valinato)palladium(II) monohydrate, $C_{10}H_{22}N_2O_5Pd$. *Cryst. Struct. Commun.* **1973**, *2*, 395–398.
74. Komorita, T.; Hidaka, J.; Shimura, Y. Metal complexes with amino acid amides. III. Geometrical structures and electronic spectra of bis(α -amino acid-amidato)palladium(II), -nickel(II), and -copper(II). *Bull. Chem. Soc. Jpn.* **1971**, *44*, 3353–3363. [CrossRef]
75. Sabat, M.; Jezowska, M.; Kozłowski, H. X-Ray Evidence of the Metal-Ion Tyrosine Aromatic Ring Interaction in Bis(L-Tyrosinato)Palladium(II). *Inorg. Chim. Acta* **1979**, *37*, L511–L512. [CrossRef]
76. Batsanov, S.S. Van der Waals radii of elements. *Inorg. Mater.* **2001**, *37*, 871–885. [CrossRef]
77. Bhowmick, S.; Bhowmick, K.C. Catalytic asymmetric carbon-carbon bond-forming reactions in aqueous media. *Tetrahedron Asymmetry* **2011**, *22*, 1945–1979. [CrossRef]
78. Zhang, G.; Luan, Y.; Han, X.; Wang, Y.; Wen, X.; Ding, C. Pd(L-proline)₂ complex: An efficient catalyst for Suzuki-Miyaura coupling reaction in neat water. *Appl. Organomet. Chem.* **2014**, *28*, 332–336. [CrossRef]
79. Rigaku Oxford Diffraction CrysAlisPro Software System. 2018. Available online: <https://www.rigakuxrayforum.com/forumdisplay.php?fid=57> (accessed on 2 June 2019).
80. Sheldrick, G.M. SHELXT—Integrated space-group and crystal-structure determination. *Acta Crystallogr. Sect. A Found. Adv.* **2015**, *71*, 3–8. [CrossRef] [PubMed]
81. Sheldrick, G.M. A short history of SHELX A short history of SHELX. *Acta Crystallogr. Sect. A* **2008**, *64*, 112–122. [CrossRef] [PubMed]
82. Dolomanov, O.V.; Bourhis, L.J.; Gildea, R.J.; Howard, J.A.K.; Puschmann, H. OLEX2: A complete structure solution, refinement and analysis program. *J. Appl. Crystallogr.* **2009**, *42*, 339–341. [CrossRef]
83. Frisch, M.J.; Trucks, G.W.; Schlegel, H.B.; Scuseria, G.E.; Robb, M.A.; Cheeseman, J.R.; Scalmani, G.; Barone, V.; Petersson, G.A.; Nakatsuji, H.; et al. Gaussian 9 Citation. Available online: <https://gaussian.com/g03citation/> (accessed on 4 May 2016).
84. Becke, A.D. Density-functional thermochemistry. III. The role of exact exchange. *J. Chem. Phys.* **1993**, *98*, 5648–5652. [CrossRef]
85. Lee, C.; Yang, W.; Parr, R.G. Development of the Colle-Salvetti correlation-energy formula into a functional of the electron density. *Phys. Rev. B* **1988**, *37*, 785–789. [CrossRef]
86. Stephens, P.J.; Devlin, F.J.; Chabalowski, C.F.; Frisch, M.J. Ab Initio calculation of vibrational absorption and circular dichroism spectra using density functional force fields. *J. Phys. Chem.* **1994**, *98*, 11623–11627. [CrossRef]
87. Andrae, D.; Häußermann, U.; Dolg, M.; Stoll, H.; Preuss, H. Energy-Adjusted Abinitio Pseudopotentials for the 2nd and 3rd Row Transition-Elements. *Theor. Chim. Acta* **1990**, *77*, 123–141. [CrossRef]

